RENEWABLE NATURAL GAS PRODUCTION VIA SABATIER REACTION

A Thesis Submitted to
the Graduate School
İzmir Institute of Technology
in Partial Fulfillment of the Requirements for the Degree of

MASTER OF SCIENCE

in Chemical Engineering

by
Cansu ÇAMLIK

July 2021
İZMİR

ACKNOWLEDGEMENTS

Firstly, I would like to express my gratitude to Prof. Dr. Erol ŞEKER, my supervisor, for his support, guide, valuable remarks and engagement through the learning process of this thesis. I also would like to express my sincere gratitude to my committee members.

I warmly express my special thanks to members of our research group for being very friendly and helpful. Sincere appreciation to Özgün DELİİSMAİL for his guidance, Emre DEĞİRMENCİ and Gökmen Oğuzcan HAMZA for their assistance and for giving technical support. This master thesis would not have been possible without motivation and belief of my dear friends; Oğuzhan AKIN and Yağmur DAĞA. I should open a special parenthesis for Emre ÜNLÜ for his intense encouragement and support throughout this study.

My deepest gratefulness goes to the ÇAMLIK family for their endless support, limitless love and motivation during my educational life. I feel very lucky to have you. Last and foremost thank to my little nephew, Atlas ÇAMLIK for giving me happiness.

ABSTRACT

RENEWABLE NATURAL GAS PRODUCTION VIA SABATIER REACTION

This study attempts to understand the effect of support basicity on Sabatier reaction and improve the performance of Ni based catalysts by introducing calcium which is known for its basicity. In accordance with this purpose, Ni-Al_2O_3-CaO catalysts were synthesized with modified sol-gel method. Effect of Ni loading, calcination temperature and calcium content were investigated. Al_2O_3-CaO supports were synthesized at three ratios as follows; 70-30 wt.%, 40-60 wt.%, 10-90 wt.% wherein Ni/Al_2O_3 catalyst was used as reference catalyst. Based on thermodynamic analysis, reaction was conducted at 400ºC and 1 atm with inlet composition of CO_2/H_2=1/4 and total volumetric flow rate of 100 ml/min.

The reference catalyst calcined at 700ºC was found to be inactive at used reaction conditions due to the presence of inactive $NiAl_2O_4$ phase. Increasing Ni loading from 1 wt.% to 10 wt.% increased both CO_2 conversion and methane selectivity. Over the catalysts calcined at the temperature of 900ºC, maximum methane yield was obtained over 10Ni-70Al-30Ca-900 as 8%. The influence of Ni loading was more pronounced for catalysts calcined at 700ºC. In 10Ni-70Al-30Ca-700 catalyst, NiO particles were smaller than 5 nm. Therefore, it is conceivable that the alumina-calcium mixed oxide support could disperse higher loadings of Ni, which could result in higher CO_2 conversion. Ca modification was found to have a prominent impact on both methane selectivity and yield. With 10Ni-10Al-90Ca-700, being best performing catalyst, CO_2 conversion obtained as 76% and methane yield was 60%. The promotion of catalytic performance might arise from intensifying the CO_2 chemisorption supported by XRD and TGA results.

ÖZET

SABATIER REAKSİYONU İLE YENİLENEBİLİR DOĞAL GAZ ÜRETİMİ

Bu çalışma, destek bazlığının Sabatier reaksiyonu üzerindeki etkisini anlamaya ve Ni katalizörlerin kalsiyum ilavesi ile performansını iyileştirmeye çalışmaktadır. Bu amaç doğrultusunda modifiye sol-jel yöntemi ile Ni-Al_2O_3-CaO katalizörler sentezlenmiş ve Ni-Al_2O_3 katalizör referans olarak kullanılmıştır. Nikel yüklemesi, kalsinasyon sıcaklığı ve kalsiyum içeriği etkisi, katalizörlerin Sabatier reaksiyonundaki performansları doğrultusunda incelenmiştir. Termodinamik analize dayalı olarak, reaksiyon koşulları CO_2/H_2=1/4 giriş bileşimi ile 400ºC ve 1 atm olarak seçilmiştir.

700ºC'de kalsine edilen referans katalizör, $NiAl_2O_4$ fazının varlığından dolayı kullanılan reaksiyon koşullarında inaktif bulunmuştur. Tüm kalsinasyon sıcaklıklarında, Ni yüklemesinin ağırlıkça %1'den %10'a yükseltilmesi hem CO_2 dönüşümünü hem de metan seçiciliğini arttırdığı gözlenmiştir. Bununla birlikte, 900ºC sıcaklıkta kalsine edilen katalizörlerde, maksimum metan verimi 10Ni-70Al-30Ca-900 üzerinden %8 olmuştur. Ni yüklemesinin etkisi, 700ºC'de kalsine edilmiş katalizörler için daha belirgin bulunmuştur. 10Ni-70Al-30Ca-700 katalizöründe, NiO partikülleri 5 nm'den küçük olarak bulunmaktadır. Bu nedenle, alümina-kalsiyum karışık oksit desteğinin, daha yüksek CO_2 dönüşümü ile sonuçlanabilecek daha yüksek Ni yüklemelerini dağıtabileceği düşünülebilir. Kalsiyum modifikasyonunun metan seçiciliği ve verimi üzerinde belirgin bir etkisi olduğu bulunmuştur. En iyi performans gösteren katalizör olan 10Ni-10Al-90Ca-700 ile %76 CO_2 dönüşümü ve %60 metan verimi elde edilmiştir. Katalitik performansın iyileştirilmesi, bazik bir destek sayesinde CO_2 kimyasal emiliminin yoğunlaşmasından kaynaklanabildiği TGA ve XRD sonuçları ile desteklenmiştir.

TABLE OF CONTENTS

LIST OF FIGURES

Figure **Page**

Figure **Page**

LIST OF TABLES

CHAPTER 1

INTRODUCTION

Global warming-induced climate change is one of the most serious environmental threats of the present time, which is widely discussed and ignored at the same time. By Intergovernmental Panel on Climate Change, global warming and consequently climate change is linked to greenhouse gas (GHG) emissions since GHGs are responsible for warming the earth's surface by creating a positive radiative force in the climate system, namely the greenhouse effect (Kırlı and Fahrioğlu 2018).

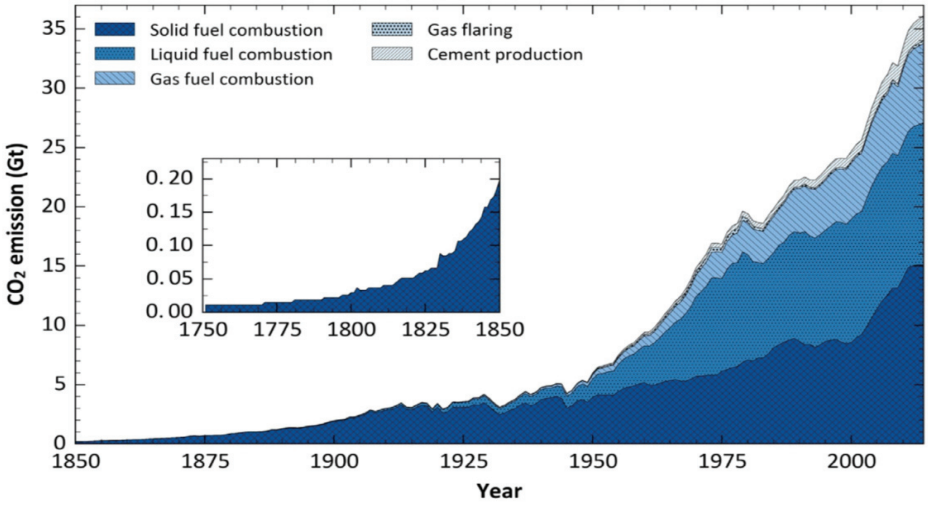

Figure 1. Annual global CO_2 emissions from 1870 to 2014
(Source: Mebrahtu; Krebs; Abate; Perathoner et al., 2019)

While carbon dioxide (CO_2) is the least hazardous GHG per kilogram emitted, it has the most adverse effects on global warming and climate change with 82% releasing share among all the other greenhouse gases; nitrous oxide (N_2O), methane (CH_4), fluorocarbons (CFs) and chlorofluorocarbons (CFCs) (M. A. A. Aziz 2015). Combustion of fossil fuels and deforestation are the main reasons for CO_2 accumulation in the atmosphere. Figure 1 reveals that annual CO_2 emissions have continually risen from increasing utilization of carbon-rich fossil fuels (coal, oil and natural gas). The statistics

have suggested that CO_2 release would reach 35.7 Gt by the year 2040. In other words, the concentration of atmospheric CO_2 which was around 280 ppm before the industrial revolution is predicted to be up to 570 ppm by the end of the century (Wei Wang 2011).

As long as fossil fuels are the dominant energy source of power generation, this increasing trend of CO_2 content in the atmosphere will inevitably keep rising. Based on the report by UNEP (United Nations Environment Programme), earth surface temperature is projected to increase by more than 2°C by 2050 and 4°C by 2100, if anthropogenic GHG emission is not altered by strict and fast global actions (Li et al. 2018). Long before, in 1895, Svante August Arrhenius calculated that doubling the amount of atmospheric CO_2 will cause a 5-6°C increment of Earth's average temperature (Mebrahtu et al. 2019). Consequently, the problems associated with global warming, which is already alarming, such as the destruction of ecosystems, the occurrence of storms, hurricanes and, floods are expected to increase further (Mebrahtu et al. 2019). Therefore, there has been mounting pressure for countries to govern emissions by developing efficient CO_2 capture and utilization systems.

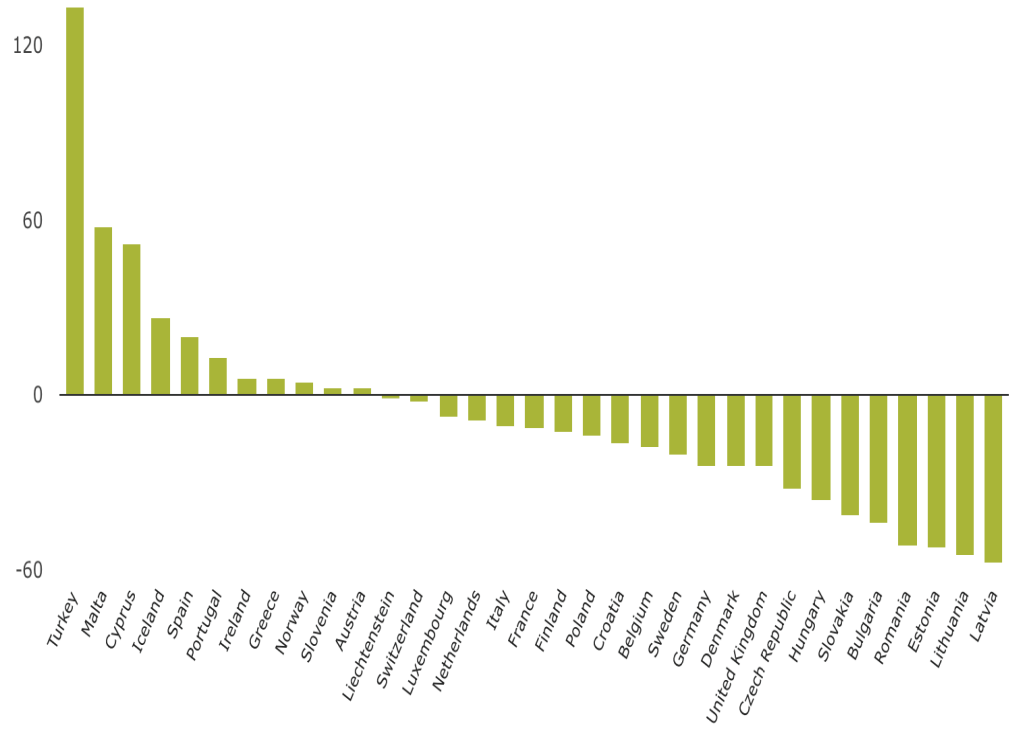

Figure 2. Change in total GHG emissions in EEA-33 countries (1990–2012)
(Source: Owusu; Asumadu-Sarkodie; Dubey, 2016)

On this subject, Paris Agreement following to the Kyoto Protocol, Copenhagen Accord and Cancun Agreements has been emerged as an international joint effort in 2015 at the United Nations Climate Change Conference (COP21) by aiming to restrict the global average temperature increment less than 2°C above preindustrial levels (Mebrahtu et al. 2019). The Agreement is based on parties' Intended Nationally Determined Contributions (INDCs) that represents each countries' national status comprising objectives for GHG emission reduction, performance-based targets and deviation from business as usual (BaU) projections. For instance, GHG emissions of Turkey increased by 133.4% (Figure 2) between 1990 and 2012 (Owusu, Asumadu-Sarkodie, and Dubey 2016) and it is ranked as the 18th largest CO_2 emitter country in 2015 (Kırlı and Fahrioğlu 2018). Within the scope of Paris Agreement, Turkey submitted its INDCs to reduce GHG emissions up to 21% from BaU level until 2030 by utilizing solar power to 10 GW, wind power to 16 GW with full hydroelectric potential (Ari and Yikmaz 2019). The fact remains that Paris Agreement may only be successful by directing present energy arrows to renewables.

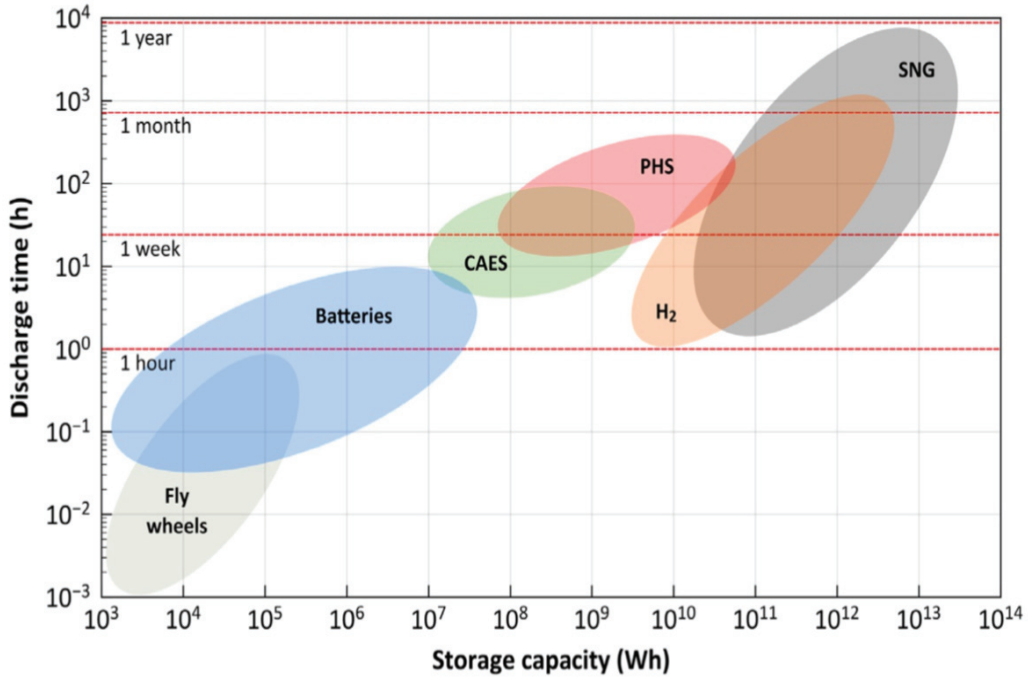

Figure 3. Charge/discharge period and storage capacity of different electricity storage systems where CAES: compressed air energy storage; PHS: pumped hydro storage; SNG: synthetic natural gas (Source:Schaaf;Grünig;Schuster;Rothenfluh et al., 2014).

In general, three possible strategies exist in order to reduce CO_2 emissions (Wei Wang 2011);

1. Reduction of CO_2 amount produced
2. Carbon Sequestration and Storage
3. Utilization of CO_2 as raw material

The best solution for managing CO_2 emission is to produce less amount of CO_2 in the first place. This strategy requires *i)* improvements of energy-efficient systems and/or *ii)* replacing fossil fuels with less carbon-intensive energy sources such as hydrogen, and renewables (e.g., bioenergy, solar energy, geothermal energy, hydropower, wind and ocean energy). Although Xiaoding et al. pointed out that using the best available technologies so that increasing current efficiency in electricity production from 30-40% to 60% may halve the CO_2 emission, from technical and economic points of view, this option might be limited (Xu Xiaoding 1996).

For later case, in despite of the great advantages of renewable energy, a certain drawback exists; the intermittency of energy generation by time of day or even seasons due to the fact that nature of many renewable energy sources is climate dependent. Moreover, there are other issues including high cost, grid connection and storage challenges. Long-term and grid-scale energy storage solutions are required due to the imbalance between renewable energy generation and instantaneous demand (Owusu, Asumadu-Sarkodie, and Dubey 2016). In 2016, the wind energy installed in Asia, Europe and the USA were 26.0, 12.9, and 4.9 GW, which cause 142.0, 134.0 and 65.9 GW wind energy accumulation, respectively. These figures reveal the urgency for the improvement of current energy storage systems (Miao et al. 2016). Excess electricity can be buffered in a variety of ways, including mechanical, potential, and chemical energy storage. These storage possibilities can be compared according to their storage capacities and charge/discharge times. As demonstrated in Figure 3, only hydrogen and synthetic natural gas (SNG) as chemical secondary energy carriers meet the requirements of high storage capacity together with high charge/discharge periods to compensate the long-term fluctuations (Schaaf et al. 2014). Methane, main component of natural gas, is more beneficial over hydrogen due to higher volumetric energy content and safety aspects. Additionally, SNG can be fed into existing gas grids through a wide distribution network (Su et al. 2016).

The second strategy in CO_2 management is Carbon Sequestration and Storage (CSS) which has been implemented to capture and store CO_2 underground or in aquifers, especially seas and oceans. Although this route offers a quick solution for cutting CO_2 emission, it suffers from several issues including the cost, safety problems related to the potential leakage of CO_2 and lack of information about long-term impact on environment, as well.

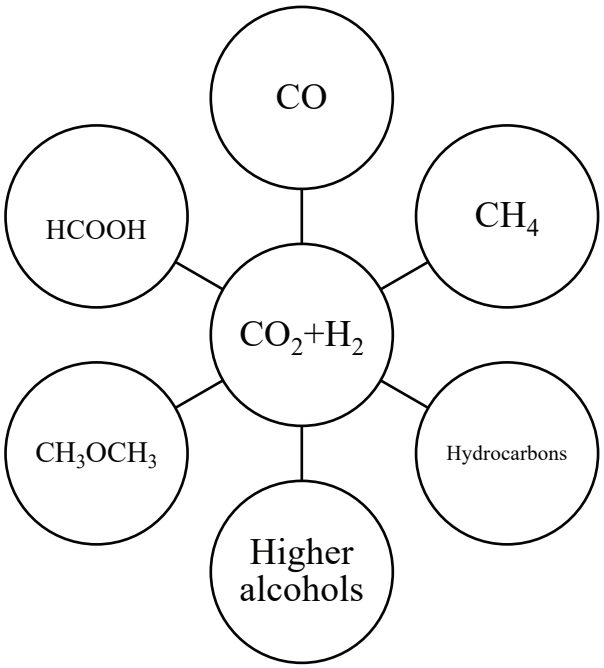

Figure 4. Hydrogenation of CO_2 to chemicals and fuels
(Source: Adapted from Wei Wang, 2011)

Last potential solution to this problem is considering CO_2 as a raw material. Captured CO_2 could be utilized and converted into fuels and chemicals offering this greenhouse gas a 'second life' (Ocampo, Louis, and Roger 2009). Currently, converted CO_2 are not even 1% of the emission (Muller et al. 2013). For the present, total global CO_2 use is below 200 million tons per year, while global anthropogenic CO_2 emissions exceed 32,000 million tons per year (Rafiee, Khalilpour, and Milani 2019). In fact, industrial processes using CO_2 as a chemical feed stock is limited to synthesis of urea and its derivatives, salicylic acid, and carbonates because of the thermodynamic stability of carbon-oxygen double bonds of CO_2. Accordingly, hydrogen, having a higher Gibbs free energy, can be used as co-reactant to transform CO_2 into fuels and chemicals including methane, methanol, ethanol and higher alcohol, hydrocarbons, dimethyl ether (DME), formic acid, formates and formamides as presented in Figure 4 (Wei Wang 2011).

By considering ever-increasing energy demand with increasing population and diminishing of the fossil fuel reservoirs, fuel production from non-fossil sources becomes the ultimate aim of humanity. In this regard, CO_2 may be seen as an attractive C1 building. Despite the fact that methanol and DME are promising fuels which can be use in internal combustion engines, high pressures (~5 MPa) are required to perform these reactions. Furthermore, complete conversion of CO_2 to methanol and DME is a difficult operation such that CO_2 conversion to methanol is still very low (<20%) (M. A. A. Aziz 2015). On the contrary, the hydrogenation of CO_2 to produce methane is more simple reaction; performable under atmospheric pressure.

Methane is the main component of natural gas, therefore methane produced from hydrogenation of CO_2 is called substitute or synthetic natural gas. SNG may be considered as an ideal fuel owing to high energy density, lower carbon footprint compared to other fossil fuels, smoke and slag-free composition. Additionally, produced methane then can be transported at low cost via already existing natural gas pipelines through a wide distribution network, as well as reconverted with high conversion efficiency by further processes.

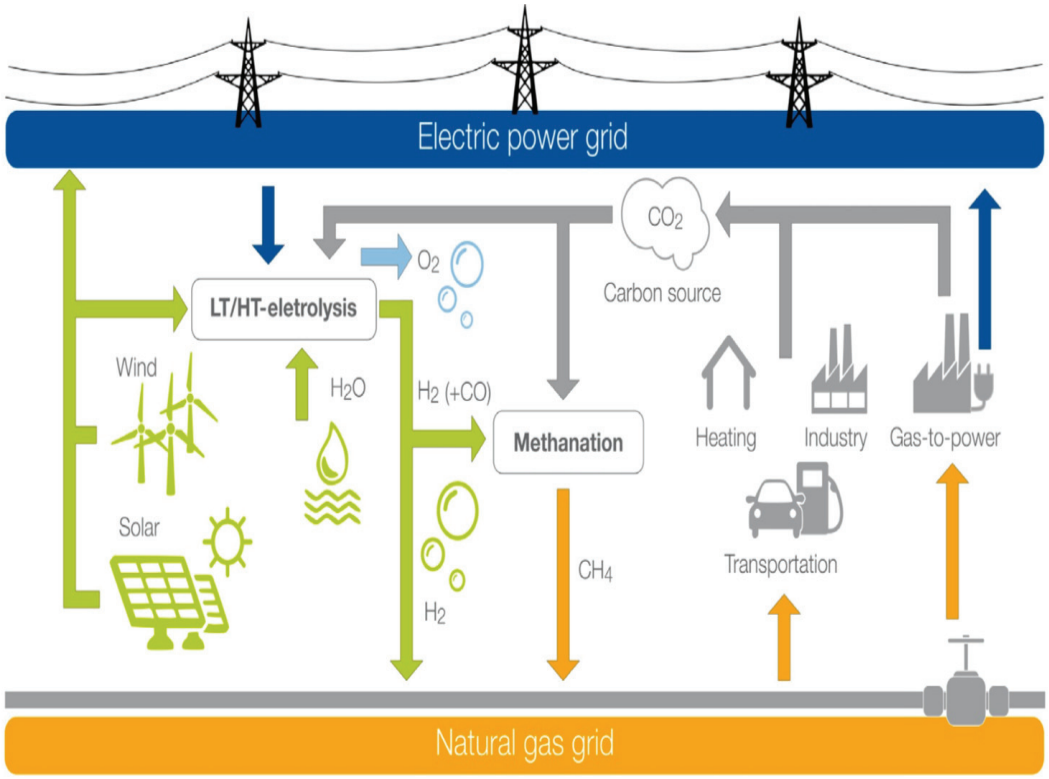

Figure 5. Overview of CO_2 methanation under PtG concept

(Source: Mebrahtu; Krebs; Abate; Perathoner et al., 2019)

One of the emerging processes for CO_2 utilization into fuels is SNG production that also allows storage and transportation of renewable energy efficiently when green hydrogen is used as co-reactant. An interlinkage between the harvested electricity from renewable energy sources and recycling CO_2 as feedstock to produce SNG becomes a prominent solution to irregular renewable energy while reducing CO_2 emission. This concept is called Power to Gas Technology (PtG). Among the storage systems presented in Figure 3, SNG is the most advantageous one in terms of both discharge time and storage capacity. In near future, it is highly possible that PtG technology may take a crucial role in long-term and large-capacity renewable energy storage.

In Figure 5, three steps of PtG technology are introduced which involves *i)* generation of renewable electricity, *ii*) renewable H_2 production by low and high temperature water electrolysis and *iii*) using green H_2 for catalytic CO_2 conversion to methane via Sabatier reaction. The essence of power-to-gas technology is to produce SNG by utilizing hydrogen that is generated from surplus renewable energy for instance energy produced from wind turbines at night when the demand is lower. SNG produced in this manner can also be named as 'renewable natural gas'. When hydrogen is provided via water electrolysis by using that excess energy from renewables and CO_2 is captured from flue gas, biomass or other carbon-containing resources, CO_2 methanation, so-called Sabatier reaction, becomes a rational approach of not only cutting CO_2 emissions but also storing renewable energy in chemical media. Moreover, large amount of carbon which is the building block of fossil fuels and petrochemicals is prevented from being wasted via CO_2 emission yielding more sustainable use of the resources without producing more CO_2. Thus, CO_2 conversion to methane as an energy carrier seems to be the most attractive and promising solution in CO_2-reduction research area by also considering today's world of high energy demand. The CO_2 to methane market is predicted to increase to between 4 billion cubic meters (pessimistic) and 65 billion cubic meters (best case) yearly by 2030 (Lee et al. 2021).

Data collected from pilot plants showed that the cost of methane produced by utilizing renewable hydrogen is several times of conventional natural gas price (Miao et al. 2016). For economic competitiveness, technical improvements on the point of efficiency are essential. Hence, developing highly active, selective and, stable catalysts is of great importance for the economic viability of large-scale energy storage facilities.

The present thesis attempts to understand the effect of support basicity on CO_2 methanation and improve the performance of Ni-based catalysts by introducing calcium which is known for its basicity. In accordance with this purpose, Ni supported on Al_2O_3-CaO mix oxide catalysts were synthesized with the modified sol-gel method. The basic strength of catalysts was arranged by preparing supports with different compositions. Al_2O_3-CaO supports were synthesized at three ratios as follows; 70-30 wt%, 40-60 wt%, 10-90 wt% with varied nickel contents (1,5,10 wt%). Ni/Al_2O_3 catalyst was used as reference catalyst. Prepared catalysts were calcinated at the temperatures of 500ºC, 700ºC and, 900ºC for 6 hours in order to investigate the effect of calcination temperature. All catalysts were tested and compared through CO_2 methanation reaction at the reaction temperature of 400ºC, inlet composition of CO_2:H_2=1:4 with a total volumetric flow rate of 100 ml/min based on the performance of the catalysts. The product compositions were analyzed by using GC-TCD and catalysts were characterized by using XRD, BET and, TGA.

This thesis consists of 5 main chapters. In the first chapter, possible strategies for reducing CO_2 emission with their advantages and disadvantages and the importance of Sabatier reaction under the power-to-gas technology are stated. In Chapter 2, literature review is presented on methanation of carbon dioxide in its aspects including the history of Sabatier Reaction, methanation catalysts, proposed reaction mechanisms and the effects of the active metal, support, additive and calcination temperature on the catalytic activity. Third chapter is about material and methods used in this thesis explaining details about the experimental procedure. In Chapter 4, results of the catalyst characterization and performed runs are presented and discussed. The final chapter includes conclusions driven from the collected data**.**

CHAPTER 2

LITERATURE SURVEY

2.1. The CO_2 Methanation: Sabatier Reaction

Catalytic hydrogenation of CO_2 to methane, Sabatier reaction, was first observed by Nobel Prize-winning French chemists Paul Sabatier in the early 1900s over a Nickel catalyst following reaction 1;

$$CO_2 + 4H_2 \leftrightarrow CH_4 + 2H_2O \quad \Delta H_{298K} = -165.0 \frac{kj}{mol} \qquad \textbf{2.1.1}$$

The most widely accepted mechanism of the methanation reaction is the combination of an endothermic reversed water gas shift (rWGS) reaction and an exothermic CO methanation reaction, as shown in reaction 2 and reaction 3, respectively (Stangeland et al. 2017).

$$CO_2 + H_2 \leftrightarrow CO + H_2O \quad \Delta H_{298K} = 41.2 \frac{kj}{mol} \qquad \textbf{2.1.2}$$

$$CO + 3H_2 \leftrightarrow CH_4 + H_2O \quad \Delta H_{298K} = -206.1 \frac{kj}{mol} \qquad \textbf{2.1.3}$$

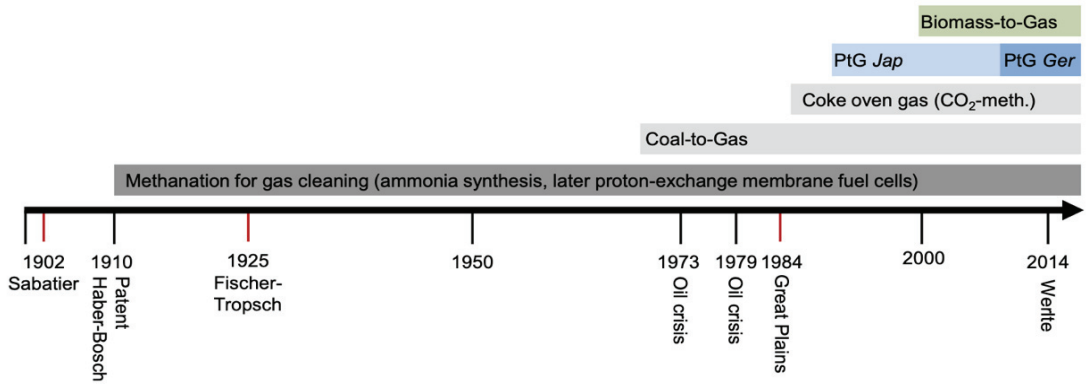

Figure 6. History of Methanation

(Source: Rönsch; Schneider; Matthischke; Schlüter et al., 2016)

As can be seen in Figure 6, the catalytic hydrogenation of CO_2 is an old and important process which was earlier used for removing trace amounts of carbon oxides from the feed gas for ammonia synthesis to avoid catalyst poisoning. Methanation reaction and catalysts regained an extensive interest in producing SNG from naphtha and coal, during the oil crisis in 1970s (Gao et al. 2015). At present, there are nearly 15 coal-to-SNG plants proposed in the U.S and more than 20 coal-to-SNG plants are in construction in China because of China's abundant coal and poor natural gas reservoirs (Gao et al. 2012). In 1980s, studies on processes subjecting CO_2 methanation attend to use of coke oven gas or furnace gas. Yet, only quite a few of those studies were successfully implemented on a commercial scale as it requires high effort for cleaning of these gasses (Rönsch et al. 2016).

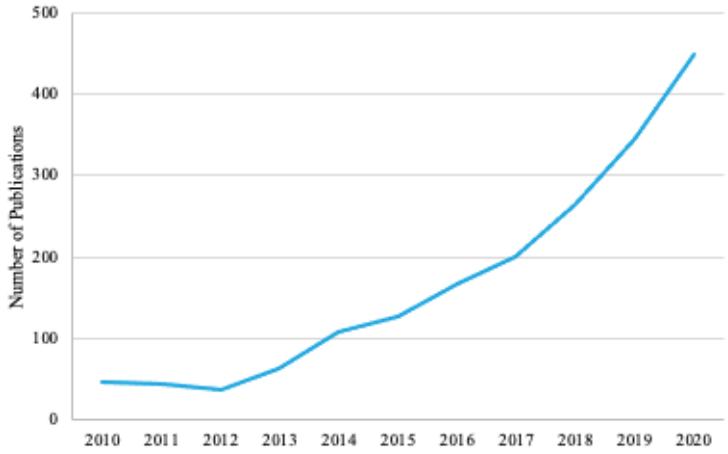

Figure 7. Number of publications dealing with 'CO_2 methanation' versus years (Source: Adapted from Web of Science)

Recently, the Sabatier reaction has received more and more attention from both the scientific community and industry due to its application in power-to-gas technology, so that the number of publications addressing CO_2 methanation has drastically increased since 2012 as introduced in Figure 7. CO_2 methanation under the PtG technology is also started to be tested in several projects. Between the years of 2009 and 2013, five projects on pilot or commercial scale were running wherein E-Gas Project (Wertle, Germany (Li et al. 2018)) was the biggest one with an installed power of 6300 kW (Wierzbicki et al. 2018).

In addition, The National Aeronautics and Space Administration (NASA) also considers the Sabatier reaction as a key technology for use in future manned space

colonization on Mars. By bringing terrene hydrogen to Mars, conversion of Martian carbon dioxide atmosphere into methane and water will be possible for fuel and astronaut life-support system (M. A. A. Aziz 2015).

2.2. Methanation Catalysts

In general, a catalyst must fulfill certain requirements such as low cost, high activity, selectivity, stability, easy recovery, and reuse for industrial usage. In terms of stability, separation, handling, and reuse, which attempts to reduce costs for large-scale production, CO_2 methanation via heterogeneous catalysts has gained the main attention over homogeneous ones.

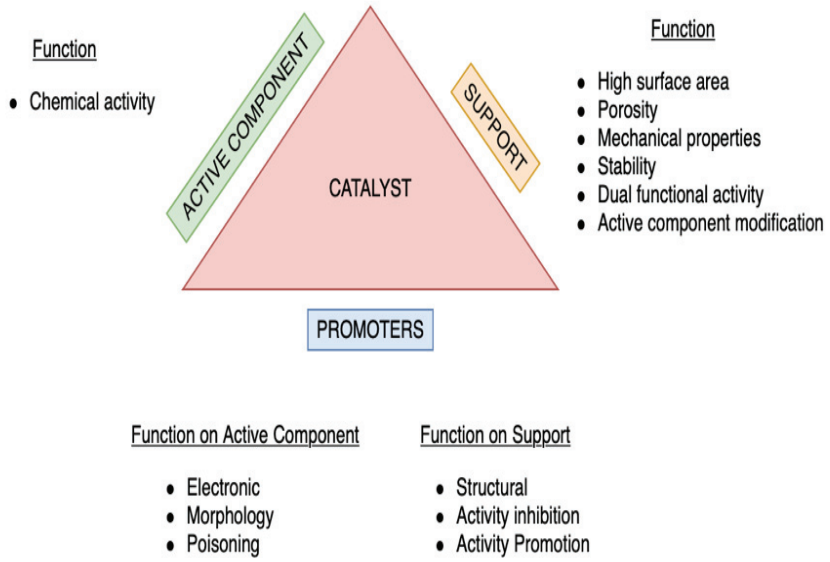

Figure 8. Catalyst components and functions
(Source: Adapted from Richardson, 2013)

Although there are some catalytic materials formed from single substances, majority of heterogeneous catalysts are made of 3 components as follows; an active component, a support/carrier and promoters. In Figure 8, function of each component was given. Since active component itself gives chemical activity to the catalytic material, choosing suitable an active component for the target reaction is the first step of catalyst design. Even though the most important function of support materials is to provide high

surface area in order to disperse active component, they are also employed to perform many functions such as porosity, mechanical properties, bifunctional activity and modification of active materials. The last component of a typical catalyst is the promoter which is added in small amounts to the catalyst formula to advance either the functions of active component or the support or both (Richardson 2013). Aside from high activity and selectivity, the prevention of catalyst deactivation is a fundamental concern in catalyst design (Seemann and Thunman 2019).

While the CO_2 methanation is thermodynamically favorable with ΔG_{298K}=-114 kJ/mol, the reduction of the fully oxidized carbon to methane is an eight-electron process causing significant kinetic limitations (M. A. A. Aziz 2015). From a thermodynamic standpoint, high CH_4 yields are limited by the equilibrium at temperatures above 225ºC for 1 atm and around 300ºC for 30 atm due to exothermic nature of the reaction (Gao et al. 2012). However, according to the dynamic theory, lowering the temperature lowers the reaction rate because of the strong C=O bonds. Thus, a catalyst is required for appropriate rates. On account of the equilibrium and kinetic limitations of the reaction, the difficulty is to develop a proper catalyst in order to achieve high activity and selectivity towards methane at moderate temperatures and atmospheric pressure. Therefore, the methanation catalyst should be active at low temperatures to ignite the reaction in SNG production process and also stable at high temperatures due to the strong exothermic reaction which may result in hot spots around 600-700ºC (Gao et al. 2015).

Extensive studies have been conducted on the hydrogenation of CO_2 toward methane using catalysts containing group VIIIB metals (Ni, Fe, Ru, Co, Rh, Ir, Pt) supported on various metal oxides (SiO_2, Al_2O_3, ZrO_2, TiO_2, and CeO_2). Ni, Ru and Rh based catalysts have proven their activity for this reaction while the rest catalyzes simultaneously side reactions (Wei Wang 2011). Based on the earlier works, the activity performance of metal-based catalysts increased in the order: Ru > Rh > Ni > Co > Pt > Pd under methanation conditions (Li et al. 2018). Noble metals show good catalytic activity for CO_2 methanation with good resistivity to sintering and coke formation. The superior low temperature (473-673 K) activities of Ru/Al_2O_3 over Ni-based catalysts is a well-established fact. It should be noted, however, that to carry out this reaction at low temperature, high Ru loadings (5-10%), very low space velocities, and excellent reactor cooling are required. When reaction temperature increased, i.e. to 673-773 K, the efficiency of Ru catalyst approaches to that of Ni catalyst because of dramatic increase in

CO selectivity. Hence, Ni-based catalysts have been the most widely investigated and proposed catalysts for carbon dioxide methanation due to their acceptable activity, 160 times lower cost and availability, despite of the fact that Ru is most selective metal towards methane (Garbarino et al. 2014). Their reasonable activity and the much lower manufacturing cost make Ni-based catalysts interesting from a commercial standpoint.

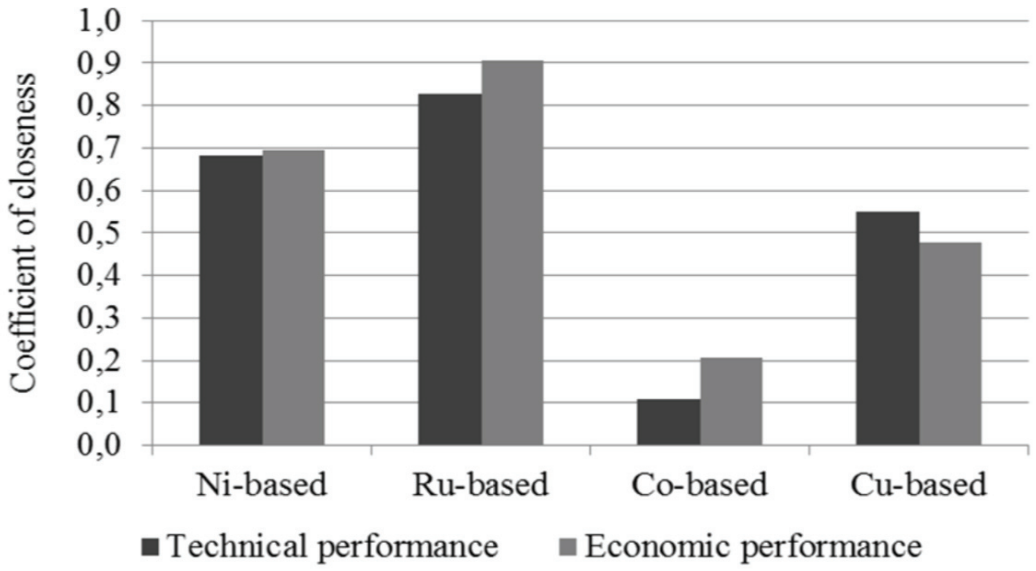

Figure 9. TOPSIS results
(Source: E. Dace, 2014)

To gain insight, Ni, Ru, Co and Cu-based catalysts were compared quantitively with respect to their technical and economic performance by using Technique for Order Preference by Similarity to an Ideal Solution (TOPSIS) (E. Dace 2014). H_2/CO_2 ratio, temperature, gas feed rate, GHSV and catalyst stability were investigated as the influencing parameters and formed the basis of the evaluation. Despite their high cost, Ru-based catalysts were found to be the catalyst with the best technical and economic results as shown in Figure 9. The essence of their efficiency lies under the fact that Ru catalysts maintain their stability over a wide range of temperature. Following to Ru-based catalysts, Ni was assigned as the second-best option for CO_2 methanation. However, technical and economic performance of Ni-based catalysts may be improved by further developments in their stability.

It is well-known that conventional nickel-based catalysts suffer from deactivation at low temperatures and heat release during the exothermic reaction (Lv et al. 2020b). Interaction of metal particles with CO and thus the formation of mobile nickel carbonyls causes metal sintering and deactivate the catalyst (Graca et al. 2014). Therefore, there is a strong need to enhance catalytic performance and stability of more abundant and cheaper Ni-based catalysts. Various studies have been conducted to improve the low-temperature performance of Ni-based catalysts for preventing deactivation and surpass the kinetic limitation by controlling particle size of Ni on support, adding of second metal or promoter to the catalyst formula and employing different support materials.

Despite the fact that various supports have been reported to be active for CO_2 methanation, Ni catalysts supported on Al_2O_3 remain the most offered formulation by some leader catalyst producers e.g. by Johnson Matthey, Topsøe and Clariant-Süd Chemie (Garbarino et al. 2014). In the study of Veselovskaya et al., elemental analysis of NKM-2V, a commercial nickel methanation catalyst, was performed by atomic emission spectroscopy and content of the catalyst was found as 23.4 wt. %Ni, 13.3 wt. %Al, 7.36 wt. %Ca, 0.57 wt. %Si (Veselovskaya, Parunin, and Okunev 2017).

2.3. Reaction Mechanism of CO_2 Methanation

A reaction mechanism is defined by elementary steps. In reaction mechanism, there are three important points to be figured out; intermediates, the rate-determining steps leading to the intermediates and active sites where the reaction proceeds (Miao et al. 2016).

Even though the methanation reaction has been known for a long time, the exact reaction mechanism for CO_2 methanation still subjects to debates mainly because of the uncertainty in determining the intermediates involved in rate determining step. Nevertheless, fully understood mechanism of Sabatier reaction will be helpful to develop desired catalyst properties such as high activity, selectivity, and durability. In order to understand the course of the reaction in more detail and thus be able to guide the catalyst design, in situ observation with various spectroscopy techniques and by computational modelling of the elementary steps has been engaged.

Although different opinions on the nature of intermediates and methane formation process exist, the overall reaction of CO_2 and CO methanation is represented by reactions

1 and 3 in section 2.1, respectively. Proposed reaction mechanisms for CO_2 methanation divide into two main categories as dissociative scheme and associative scheme (Figure 10). The first and most accepted path starts with the dissociative adsorption of CO_2 to form CO on the catalyst surface prior to methanation. Then, it proceeds same as CO methanation. It should be noted that there is still no consensus on CO methanation mechanism, either. In the second proposed mechanism, reaction is believed to be proceed by the direct hydrogenation of CO_2 to methane via carbonate or formate intermediates without the formation of carbonyl (Wei Wang 2011).

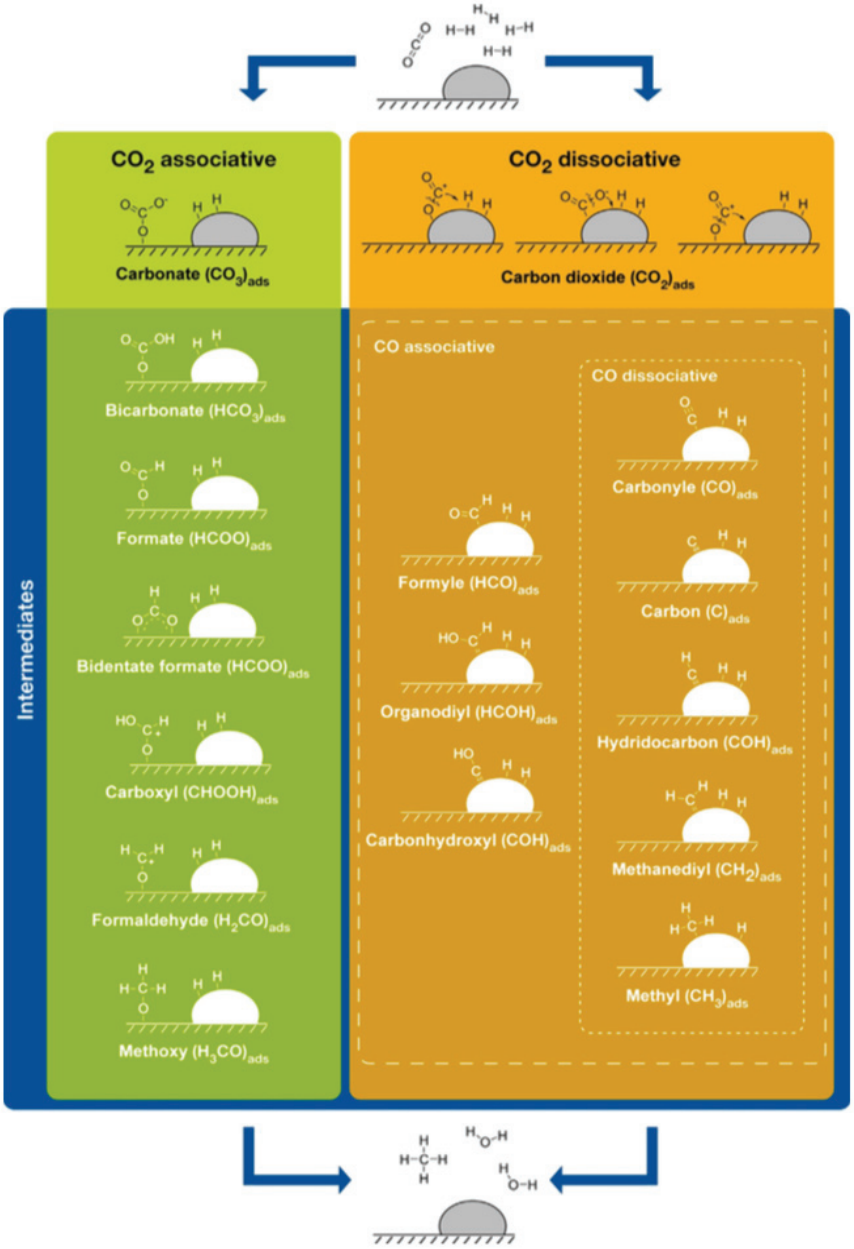

Figure 10. Reaction mechanism of CO_2 methanation
(Source: Mebrahtu; Krebs; Abate; Perathoner et al., 2019)

In CO_2 methanation, rate-determining step is suggested as either the formation of oxygenates (CH_xO) and their hydrogenations or the formation of surface C in CO dissociation and its reaction with hydrogen. Proposed reaction mechanisms of CO_2 methanation were explained in the following subsections 2.3.1 and 2.3.2.

2.3.1. CO_2 Dissociative Methanation

In CO_2 dissociative methanation route, CO_2 from the gas phase adsorbs and dissociate into carbonyl and an oxygen atom. It is claimed that direct C-O bond cleavage is possible at low-coordinated sites such as step and kink sites. Therefore, carbonyl $(CO)_{ad}$ and $(O)_{ad}$ involve as reaction intermediates. When $(CO)_{ad}$ is formed, the reaction proceeds same as CO methanation mechanism which can be grouped as associative (H_2 assisted scheme) and dissociative (direct CO splitting scheme) which means $(CO)_{ad}$ subsequently hydrogenated or further dissociated into surface $(C)_{ad}$ and $(O)_{ad}$ (Mebrahtu et al. 2019).

Surface science approach by using model systems are employed to understand the mechanistic aspects of the reactions. Herein, Ni single crystals have been used as models in place of practical catalystys for methanation. One of those studies was conducted by Peebles et al. on Ni(100) surface. The study supports the dissociative mechanism with CO intermediate due to the proximity between the calculated activation energies for CO_2 methanation (88.7 kj/mol) and CH_4 formation from CO (72.8-82.4 kj/mol) under identical reaction conditions (Wei Wang 2011).

To provide insights into the CO_2 methanation mechanism, a recent study on CO_2 hydrogenation was conducted over a series of metals (Pd, Rh and Ni) supported on various metal oxides (SiO_2, Al_2O_3 and CeO_2) and two kinds of aluminosilicate (ZSM-5 and MCM-41) (Martin et al. 2017). Among prepared catalysts, Rh/Al_2O_3, Rh/CeO_2 and Ni/CeO_2 were further investigated due to their outperformance. In situ diffusive reflectance Fourier transform infrared spectroscopy was employed to reveal the surface interactions of CO_2 and H_2 at the range of 250-400°C. It is proposed that adsorption and dissociation of CO_2 occurs over the Rh/Al_2O_3 catalyst in the presence of H_2, resulting in the formation of linear Rh–CO species, while formates and carbonates are formed as intermediate species over the CeO_2 supported Ru and Ni catalysts. So, Martin et al.

concluded that support material may be a part of and promote the hydrogenation reaction leading different reaction intermediates (Martin et al. 2017).

2.3.2. CO_2 Associative Methanation

In CO_2 associative methanation route, CO_2 adsorbs associatively and react with adsorbed hydrogen atoms to form oxygenates and then gets hydrogenated to methane in subsequent steps. This route separates from dissociative CO_2 mechanism as no CO intermediate is formed. It is claimed that barrier for C-O bond splitting is lowered by the presence of hydrogenated intermediates.

This route starts with adsorption of CO_2 from the gas phase as carbonate $(CO_3)_{ad}$ on the support, following that $(CO_3)_{ad}$ turns into oxygenates such as bicarbonate $(HCO_3)_{ad}$, formate $(HCOO)_{ad}$, and formyl $(CHO)_{ad}$ by hydrogenation (Mebrahtu et al. 2019). In hydrogenation steps, the adatoms of $(H)_{ad}$ are believed to be provided by the metal particles. Since gaseous dihydrogen is dissociated on the Ni-particles and adatoms are transferred to the support to react with carbonate, the metal-support interface is regarded as the active sites.

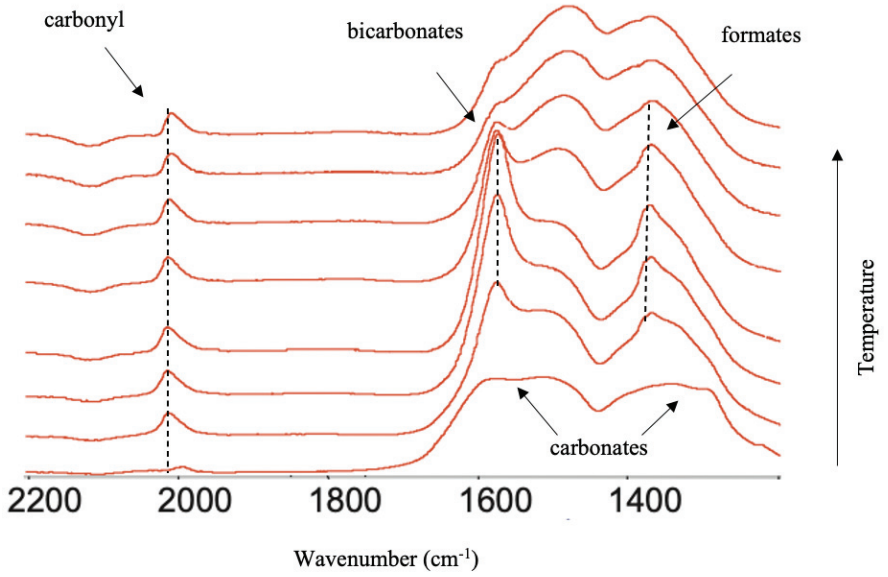

Figure 11. FTIR spectra for CO_2 methanation on the Ni–ceria–zirconia catalyst (150 to 400°C, H_2:CO_2 = 4:1) (Source: Aldana; Ocampo; Kobl; Louis et al., 2013)

Aldana et al., one of the associative CO_2 mechanism supporter research group, asserted that main mechanism for CO_2 methanation does not require CO as reaction intermediate and metal-support interaction is the key parameter. In order to understand the role of CO in the global reaction, Ni supported on ceria-zirconia (Ni-CZ) mixed oxide support was chosen as catalyst and compared with conventional Ni-SiO_2 catalyst through Sabatier reaction. Carbon dioxide methanation was conducted in a fixed-bed down-flow reactor at 350°C and atmospheric pressure where H_2 and CO_2 were mixed at a stoichiometric ratio of 4:1. In despite of lower surface area of Ni-CZ (3.1 m^2/gr), a better catalytic activity was achieved than Ni-SiO_2 (8.1 m^2/gr). Thus, IR operando measurements have been carried out for further discrimination. The FTIR spectra for CO_2 hydrogenation at 150°C indicated that carbonate was located on the support and carbonyl on the Ni metal for Ni-CZ catalyst. With increasing temperature, carbonate hydrogenated to bicarbonate and then bicarbonate dehydrated to formate species very quickly whereas carbonyl bands on Ni do not undergo any change as shown in Figure 11. Results from the transient experiments evidenced that on the Ni-ceria-zirconia catalysts, CO is not produced as a consequence of formate or carbonate hydrogenation mechanism nor it appears in the course of methane formation. CO is probably showed up through a redox cycle of CO_2 on Ce^{+3} sites in a parallel pathway. Therefore, H would be split on Ni^0 sites and CO_2 would be activated on the ceria-zirconia support to form carbonates and then hydrogenated into formates. On the contrary, Ni-SiO_2 analysis of the outlet gas composition produced very fast response to the changes in feed gas showing that silica support has no additional role other than to disperse active phase. Moreover, a strong relation between the bands corresponding to carbonyls on Ni^o and methane formation was observed for Ni-SiO_2 which might indicate that CO_2 dissociates on the metallic surface competitively with H_2. It explains nearly 5 times higher value of TOF of Ni-CZ catalyst where CO_2 and H_2 were activated at the different sites of the catalyst. The CO_2 associative methanation mechanism involves basic sites of the support for CO_2 adsorption. Thus, interaction between Ni and basic support becomes a key parameter (Aldana et al. 2013).

In another study conducted by Pan et al., formate species are regarded as major intermediate for methane production as methane formation is increased at the expense of formate signal from in situ FTIR spectroscopy on Ni–ceria catalyst (Miao et al. 2016).

However, this argument is rejected by Upam et al. due to the reason that a formate would not be stable at the methanation temperature. They proposed that CO_2 methanation

does not take place through a CO intermediate nor a formate intermediate, but it is associated with surface carbonates on Ru doped-ceria catalyst. Experiments showed that most of the carbonates are spectators and only a minority of those species involves methanation by reacting with H_2. Indeed, the degree of reduction of the surface determines the type of surface carbonates present. Thus, catalyst activity depends on the degree of surface reduction. It was found that too reduced or too oxidized catalyst surfaces lost their activity towards methanation. Hence, the mechanism that proceeds through the CO_2 dissociation followed by CO reduction was found far from realistic for $Ru_{0.05}Ce_{0.95}O_{2-\delta}$ catalyst (where δ varies with the degree of reduction) since $CO+H_2$ exposing causes reduction of catalyst and makes it inactive. Such a feed contains two reductants would produce no methane. Instead, species containing carbon, one oxygen atom and some hydrogen were suggested as reaction intermediates (Upham et al. 2015).

Besides of experimental studies, a DFT (density functional theory) study was conducted on CO_2 methanation on Ni-alumina system. Activation energy of both associative and dissociative routes were calculated by Pan et al. It was found that the pathway is altered by surface hydroxyl $(OH)_{ad}$. By varying the reaction conditions, partial pressure of by-product water and thereby surface coverage of hydroxyl can be tuned. When the catalyst surface is hydroxylated, the dissociative route became kinetically and thermodynamically favorable (E_a= 0.69 eV). If hydroxyl is not available, formate became the major intermediate (E_a= 1.25 eV) (Miao et al. 2016). It is stated that higher coverage of surface hydroxyls leads to more selective methane formation through rWGS reaction rather than through formate species. However, uncontrolled amount of surface hydroxyls on oxide causes destabilization of the catalyst by lowering the metal-support interaction (Pan, Liu, and Ge 2010).

In general, the mechanism of carbon dioxide methanation is still under debate as with or without carbon monoxide intermediate. In literature, difference in observed mechanism may be attributed to reaction temperature, H_2/CO_2 ratio and the nature of catalyst employed including aspects of active metal, support and promoters. Thus, further investigations are required to reach a solid conclusion which makes catalyst optimization possible (Miao et al. 2016). At this point, model catalyst testing would be convenient due to the elimination of support and promoter material effects.

2.4. CO_2 Methanation Over Ni-Based Catalysts

The performance of catalyst toward Sabatier reaction is affected by various factors such as the effect of nickel loading, effect of support material, the effect of additives and the effect of the preparation method (M. A. A. Aziz 2015). In literature, the dispersion of active component and the metal-support interactions were found to be key factor in CO_2 methanation reaction, and they are greatly related to the preparation method and formulation of the catalysts. Preparation procedure of supported catalysts have also great influences on textural properties such as surface area, pore structure and bulk density as well as on its surface basicity and reducibility.

2.4.1. Effect of Nickel Loading

Recently, the influence of Ni loading on the performance of methanation catalysts was reviewed by Lv et al (Lv et al. 2020). Generally, nickel is supported on well-defined porous structures to increase the metallic nickel dispersion. Considering that the reaction occurs on the surface of the catalysts, dispersion of the metallic nickel might have predominant impact on the catalytic activity. Loading amount of nickel determines the coverage of support and the amount of metallic nickel sites available for the reaction which makes it one of the most influencing parameters in catalyst design. Within a defined range, the catalytic activity can be enhanced by increasing Ni content due to increasing number of active centers. Furthermore, the amount of metal loaded on the catalyst may have an effect on its reduction property (Lv et al. 2020). As mentioned before, Martin et al concluded that supports may not be inert but a factor on catalytic performance (Martin et al. 2017). Consequently, nickel loading also has impacts on the surface properties of the support which further influences the catalytic behavior in methanation via metal-support interaction and intermediates formed (Zhang et al. 2019). Yet, the effects of nickel loading on the surface status of support have not been fully understood.

Recently, Zhang et al. conducted a study to investigate the effects of nickel loading on the properties of the support and reaction intermediates. Several Ni/Al_2O_3 catalysts with varied nickel loading from 2.5 to 50 wt.% were prepared by wetness

impregnation method and tested through CO_2 methanation in a fixed bed reactor in the temperature range of 250°C-600°C. Effect of nickel loading was found substantial on both physicochemical properties and catalytic performance of the catalysts. Loading of more nickel led to a significant decrease in specific surface area, while nickel particle size was not affected significantly up to 37.5 wt.% loading. It was reported that this might arise from two reasons; alumina's mesoporous structure was able to well disperse metal species and/or strong interaction between nickel and support inhibited the agglomeration of nickel particles. With further increase of nickel loading, larger nickel particles formed as alumina has limited number of sites that could make strong interaction with nickel. Increasing nickel loading led to increase in portion of nickel having medium-strong interaction with alumina in addition with that medium and strong CO_2 adsorption peaks became more dominant which enhances activity for the reaction. The amount of nickel loading had significant effect on its catalytic efficiency; for example, a low nickel loaded catalyst (around 2.5 percent) showed poor activity towards methanation but catalyzed the rWGS reaction. They found that in the case of low nickel loading, the reverse water gas shift side reaction was competitive with the CO_2 methanation reaction. As the Ni loading increased, CO_2 methanation reaction gradually became dominant over rWGS. Hence, it is concluded that high nickel loading (around 25%) was beneficial to the enhancement of the CO_2 methanation reaction (Zhang et al. 2019).

On the other hand, Garbarino et al. carried out a study to investigate the hydrogenation of carbon dioxide into methane over Ni/Al_2O_3 catalysts with varied nickel loadings of 14, 28, 56 wt.%. They found that when Ni amount exceeds a certain level, raising it further would result in larger Ni particles which yields the higher CO production. According to the research, the catalytic behavior of Ni-based catalysts for methanation and rWGS was influenced by Ni loading and also by the redox state of Ni species. The catalysts having cubic Ni metal nanoparticles in the range of 10-30 nm resulted in methane formation with 100% selectivity with no CO formed. However, their previous findings showed that unsupported Ni nanoparticles were inactive for Sabatier reaction despite of having a particle size of 8 nm. It was suggested that the interaction of Ni particles with support was crucial for CO_2 conversion into methane. It appeared that the presence of Ni metal particles was required to activate hydrogen, but Ni species strongly interacting with the support material were likely essential to activate CO_2 and/or to prevent CO intermediate desorption from the surface of the catalyst, yielding rapid

methanation. Thus, small size Ni metal particles and their involvement in metal/support interfaces could lead strong CO adsorption which give selective methanation reaction and suppress rWGS activity. When Ni loading exceeds the theoretical monolayer coverage of support area, the selectivity to methane was decreased. Therefore, it seems likely that larger Ni particles, due to higher Ni loading, generated plain faces where rWGS may occur and CO desorbs from those sites before methanation took place. It was concluded that the location of active sites for CO_2 and CO methanation were on the edges of Ni particles and/or at the Ni/alumina interface whereas extended Ni metal faces prompt to rWGS reaction (Garbarino et al. 2014).

2.4.2. Effect of Support

Supported catalysts are produced for many reasons in order to meet the potential applications and requirements of heterogeneous catalysts such as achieving bifunctionality, obtaining high dispersion of active phase, attaining better diffusion of gases in reactors, better thermal conductivity and enhanced catalytic properties arise from metal-support interaction (Hutchings and Védrine 2004). As the skeleton of catalyst, support is a material on which active component is deposited. The active centers can be accommodated in a highly dispersed state since the support material is typically a solid with a large specific surface area and large pore volumes. The density, nature, and accessibility of active sites are primarily determined by support materials. Hence, the support has significant effect on the properties of adsorption and catalysis (Su et al. 2016). As previously stated, Garbarino and his coworkers highlights the promoting effect of the support as the unsupported active component by itself was found to be inactive (Garbarino et al. 2014). This promotion effect may arise from the electron transfer between the support and active component which increases the electron density in the metal. These electrons can improve the coupling between nickel and carbon allowing for carbon oxygen double bond splitting and selective methane production. Besides, a support with strong alkalinity could enhance CO_2 chemisorption and activation, thus providing quick reaction over the catalyst with lower carbon deposition (Lv et al. 2020).

Hydrogenation of CO_2 toward methane has been investigated over Ni catalysts with various single type of oxide supports, such as Al_2O_3, TiO_2, SiO_2, ZrO_2, and so on (Wei Wang 2011). According to the literature, the performance rating of support materials

is challenging, because interactions with the active component are dependent on a variety of variables, such as the calcination temperature (Seemann and Thunman 2019). However, it is possible to conclude that the support itself takes a role in CO_2 activation so that influences the performance of the catalyst. Different support materials exhibited significant change in methane yield at the exact same reaction conditions. For Ni containing catalysts, the impact of carrier on methane yield was stated to be 25% for MgO support and 92% for CeO_2 support (Tada et al. 2012). Adsorption of acidic CO_2 on the basic sites of supports is found more favorable. Although there is contradiction on which strength of basic sites are responsible for catalytic improvement, literature agreed on that basic sites on support plays an important role.

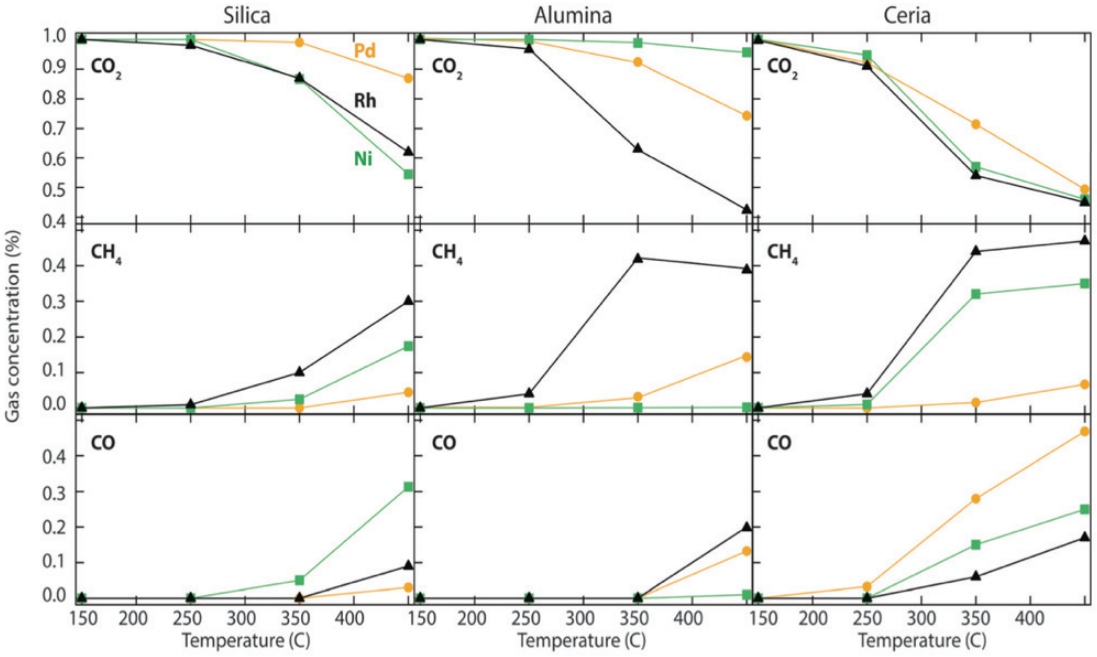

Figure 12. Outlet concentrations of methanation reaction as a function of temperature over silica, alumina and ceria supported Pd, Ni and Rh catalysts (Source: Martin; Velin; Skoglundh; Bauer et al., 2017)

Martin et al. published an extensive study on CO_2 hydrogenation at ambient pressure over Pd, Rh and Ni catalysts supported on different metal oxides; Al_2O_3, SiO_2 and CeO_2 and aluminosilicates; ZSM-5 and MCM-41 for CO_2 methanation (Martin et al. 2017). Primary aim of the study was to compare prepared catalyst through atmospheric pressure CO_2 hydrogenation by means of suppressing the rWGS and favoring methane formation. Results of ZSM-5 and MCM-41 catalyst were not reported because of very

poor catalytic activity under specified reaction conditions. Figure 12 clearly reveals the temperature dependence of the CO_2 hydrogenation. Although silica supported catalysts had the highest surface area (310-315 m^2/g) in comparison with alumina and ceria, they produced the least methane which was attributed to larger particle sizes. On the other hand, metal XRD peaks were not observed for ceria supported catalyst implying very small or amorphous metal particles and the highest CO_2 transformation to methane was observed with ceria supported catalysts followed by alumina supported catalyst. The highest CO_2 conversion to methane was obtained with Rh supported on Al_2O_3 and CeO_2, after that Ni/CeO_2. Furthermore, during transient hydrogenation of CO_2 experiments, different intermediates were observed over Rh/Al_2O_3 and Rh/CeO_2 suggesting that support material participates in CO_2 adsorption. The DRIFTS study presented in their work showed that reaction mechanism of methanation reaction over alumina support resulted in linear Rh–CO species formation, while CO was formed via formate and carbonate intermediates over the ceria supports. The paper concludes that hydrogenation process was affected significantly by both support material and reaction temperature.

2.4.3. Effect of Additives

Inherently, Ni-based catalysts suffer from some drawbacks including poor low-temperature activity and significant thermal sintering at high temperatures. As mentioned before, Sabatier reaction is thermodynamically favorable at lower temperatures but also leads to hot spots due to its exothermic nature. Therefore, it is still a challenge to develop Ni-based catalysts which are active at low temperatures to ignite the reaction in methane formation and also stable at high temperatures due to the strong exothermicity of the Sabatier reaction. The use of catalytic dopants has been considered as one of the most promising approaches addressing drawbacks of industrially-in-demand Ni-based catalysts (Lv et al. 2020).

Alkaline earth metal oxides, transition metals, rare earth metal oxides, and noble metals are the most common types of single additives for Ni-based catalysts. In addition to the particle size effect and metal-support interaction, the surface properties also play an important role on catalytic performance. It was widely believed that CO_2 adsorption and dissociation are the first step in mechanism of CO_2 methanation and CO_2 dissociation into CO through rWGS is suggested as having competitive effect to hydrogen adsorption.

In order to enhance catalytic activity, it is a necessity to increase hydrogen supply at the surface by providing fast CO_2 dissociation or direct CO_2 methanation (Yang, Feng, and Chu 2016). By introducing catalytic dopants, surface basicity can be tuned in order to improve adsorption and activation of CO_2 molecules (Li et al. 2018).

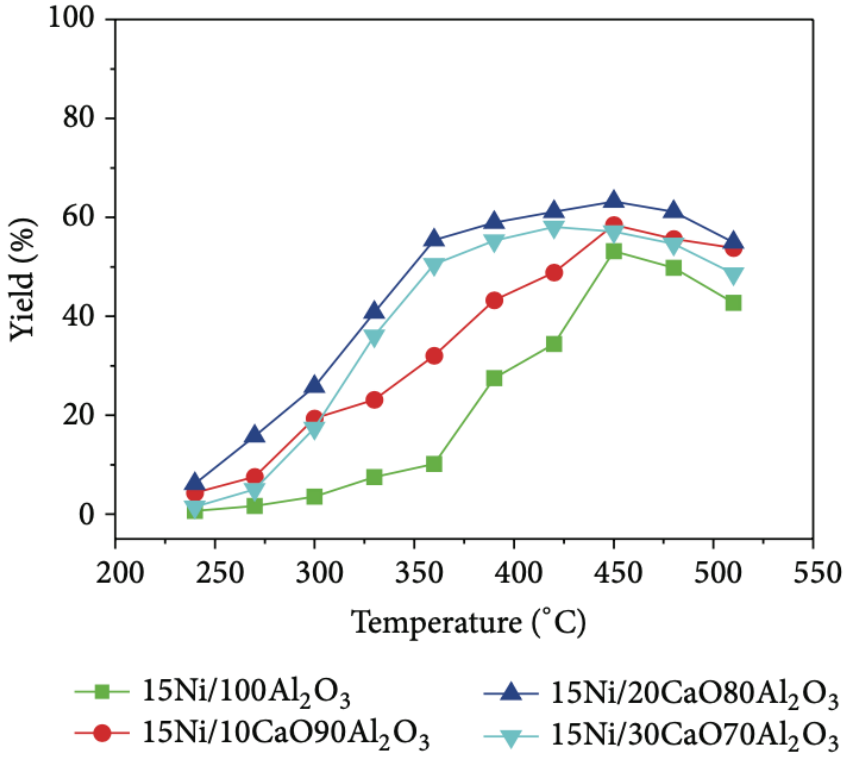

Figure 13. Methane yield versus reaction temperature over the catalysts (Source: Yang; Feng; Chu, 2016)

Alkaline earth metal oxides, such as MgO, CaO, SrO, and BaO, are known as structural additives that can significantly increase the surface basicity and consequently enhance the activity of the catalyst for CO_2 methanation (Lv et al. 2020a). Yang et al. investigated the influence of CaO-Al_2O_3 support and CaO content on the catalytic performance of Ni-based catalysts in CO_2 methanation reaction. Performance of 15Ni/100Al_2O_3, 15Ni/10CaO90Al_2O_3, 15Ni/20CaO80Al_2O_3 and 15Ni/30CaO70Al_2O_3 catalysts were performed in a temperature range of 250-500°C. XRD patterns showed that peak intensities of NiO phase were weakened for CaO added catalyst indicating improved dispersion of NiO nanoparticles. H_2-TPD indicated that high-temperature peak centered at 250-550°C means no strong interaction between metal particles and support were formed. H_2-TPR results indicated that CaO addition favored the formation of more

readily reducible NiO species as reduction temperature was shifted from 435°C to lower temperatures. From Figure 13, it can be deduced that CaO modification improved catalytic activity so that 15Ni/20CaO80Al_2O_3 exhibited methane yield of 63.2% whereas alumina supported Ni catalyst without CaO addition possess methane yield of 53.1% at 450°C. Moreover, it was seen that CaO content has an appropriate amount in catalytic performance as 15Ni/20CaO80Al_2O_3 was found superior to 15Ni/30CaO70Al_2O_3 under applied reaction conditions. Beneficial effect of CaO for catalytic activity in low-temperature region was attributed to the strength of catalyst basicity determined by CO_2-TPD. For 10 and 20 wt.% CaO added catalyst, the second low-temperature desorption peak at 350°C were observed with that of 15Ni/20CaO80Al_2O_3 being more pronounced. Among tested catalyst, 15Ni/20CaO80Al_2O_3 also showed better stability in CO_2 methanation; CO_2 conversion decreased from 66.6% to 53.7% for 360 minutes on stream at 450°C. Results were compared with CeO_2 and La_2O_3 added catalysts in literature. It was noted that, although those modifications displayed higher methane yields even at lower temperature (ca. 350°C), CaO modification was considered more beneficial owing to relative low price and approximate promotion effect to unmodified catalyst (Yang, Feng, and Chu 2016).

In Xu et al.'s previous study, compared to commercial alumina support, NiO-Al_2O_3 ordered mesoporous catalysts were found to exhibit better catalytic activity and stability due to homogenously embedded Ni particles among the alumina matrix namely confinement effect. In their recent work, aim was further improvement of low-temperature catalytic activity of ordered mesoporous Ni-Al catalyst by using a basic promoter. Ca was doped into ordered mesoporous Ni-Al composite oxide with 0,1,3,5,8 and 10% Ca/Al molar ratios at fixed Ni/Al ratio of 10% by the one-pot evaporation induced self-assembly (EISA) strategy. Fabricated catalysts were tested through CO_2 methanation reaction at varying reaction temperatures from 200°C to 450°C. H_2-TPR results showed that there was no reduction peak in the range of 300-500°C as seen in the study of Yang et al., but all catalysts irrespective of their content exhibited one explicit hydrogen reduction peak between 765-825°C indicating strong interaction between Ni particles and mesoporous framework. CO_2-TPD revealed that the surface basicity of the catalysts was dramatically increased by doping Ca modifier into the mesoporous system which is conductive to CO_2 chemisorption. As a result, apparent activation energy of the CO_2 methanation decreased from 75.2 kj/mol to 53.6 kj/mol by the presence of Ca. At

each reaction temperature, CO_2 conversion increased with increasing Ca/Al ratio up to 8% and further increase to 10% resulted in conversion decrease suggesting that only a proper amount of Ca dopant would maximize the catalytic activity. However, both low-temperature activity and CH_4 selectivity over Ca doped catalysts greatly improved compared to pristine Ni-Al catalysts. The role of basic promoter was found more pronounced at low temperatures, and conversion difference with and without Ca modification became negligible after 350°C. In contrast to Yang et al. study, no substantial deactivation of neat or modified ordered mesoporous Ni-Al catalyst were observed due to confinement effect that suppress thermal sintering of Ni particles (Xu et al. 2017).

2.4.4. Effect of Calcination Temperature

In general, physicochemical properties and catalytic activity of a catalyst are defined by its preparation conditions. Specifically, catalytic performance of Ni-based catalysts is related to its preparation method, Ni loading and calcination temperature. It is well-known that calcination temperature is one of the most affecting parameters of catalytic performance. It influences the position and the type of metallic Ni particles on support and further the porosity of the catalyst.

During the calcination process, the structure of the catalyst would be damaged, particularly at high temperatures. As a result of the thermal shrinkage of the structure, the pore size of the catalyst decreases as the calcination temperature rises. In most cases, a lower calcination temperature is preferable in order to prevent Ni species agglomeration because increased calcination temperature reduces the dispersion of Ni species, resulting in poor catalytic activity. Nevertheless, catalytic activity may be improved with increasing calcination temperature due to the fact that Ni particles could migrate from outer surface to interior (Lv et al. 2020).

The effect of calcination temperature on catalyst activity and selectivity in methanation were reported in literature. Rahmani et al. prepared a series of Ni catalysts supported on mesoporous nanocrystalline Al_2O_3 with various Ni contents by wet impregnation method. Calcination process was conducted at different temperatures. It can be seen from Figure 14 that increasing calcination temperature from 450°C to 650°C caused a significant decrease in CO_2 conversion due to lowering surface area to disperse

Ni species and growing crystalline diameter of NiO from 18.9 nm to 29.5 nm. Furthermore, XRD patterns showed that as the calcination temperature increased, the proportion of inactive $NiAl_2O_4$ phase increased. Hence, from H_2-TPR profiles, reduction peaks shifted toward higher temperatures with increasing calcination temperature (Rahmani, Rezaei, and Meshkani 2014). The results were consistent with those of Zhang et al., where reduction degree of the catalyst gradually decreased as the calcination temperature increased from 600°C to 1000°C (Lv et al. 2020). It can be concluded that crystal structures change subsequent to an increment in calcination temperature.

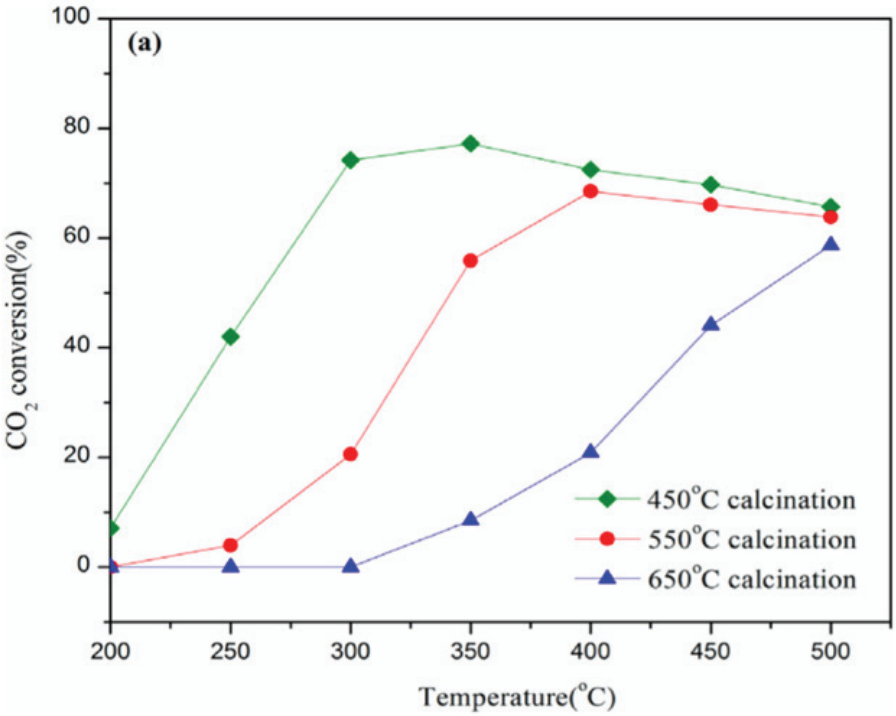

Figure 14. Effect of calcination temperature on CO_2 conversion, $20Ni/Al_2O_3$, GHSV = 9000 ml/gcat h, H_2/CO_2 molar ratio = 3.5 (Source: Rahmani; Rezaei;Meshkani, 2014).

CHAPTER 3

MATERIALS AND METHODS

3.1. Materials

In this study, Ni catalysts supported on aluminum-calcium mixed oxide were prepared with three different nickel loadings of 1, 5, 10 wt.%. Aluminum-calcium oxide support ratio was 70-30 wt.%, 40-60 wt.% and 10-90 wt.%, respectively.

In the synthesis of catalysts, alumina isoproproxide and calcium nitrate tetrahydrate were used as precursors of aluminum and calcium oxide. Nickel acetate was used as nickel source. Deionized water was used as solvent and 65 vol.% nitric acid (HNO_3) as peptizing agent in sol-gel method. Properties of used chemicals during synthesis were listed in Table 1.

Table 1. Properties of used chemicals in synthesis

Material	Chemical Formula	Molecular Weight	Purity
Alumina Isopropoxide	$Al(C_3H_7O)_3$	204.24	0.98
Water	H_2O	18.02	1
Nitric Acid	HNO_3	63.01	0.65
Calcium Nitrate Tetrahydrate	$Ca(NO_3)_2.4H_2O$	236.15	0.99
Nickel Acetate	$C_4H_6NiO_4$	176.79	0.99

3.2. Methods

Experimental part of the study includes four parts; catalyst preparation, catalytic test, product analysis and catalyst characterization. In following subsections, detailed procedure of catalyst's synthesis, testing, calculations and characterization were given.

3.2.1. Catalysts Preparation

In the present study, 27 different nickel-based catalysts were prepared by modified sol-gel method developed by Prof. Dr. Erol Şeker. For Ni-Al_2O_3-CaO catalyst synthesis, firstly, alumina sol was prepared in a 500 ml-laboratory bottle. In order to prepare alumina sol, required amount of alumina isoproproxide (AIP) was dissolved in deionized water with 1/10 g/ml ratio and stirred at 85°C for 1 hour at 400 rpm. Then, needed nitric acid was added drop wise with a certain HNO_3/Al molar ratio to the solution and mixed for 1 hour.

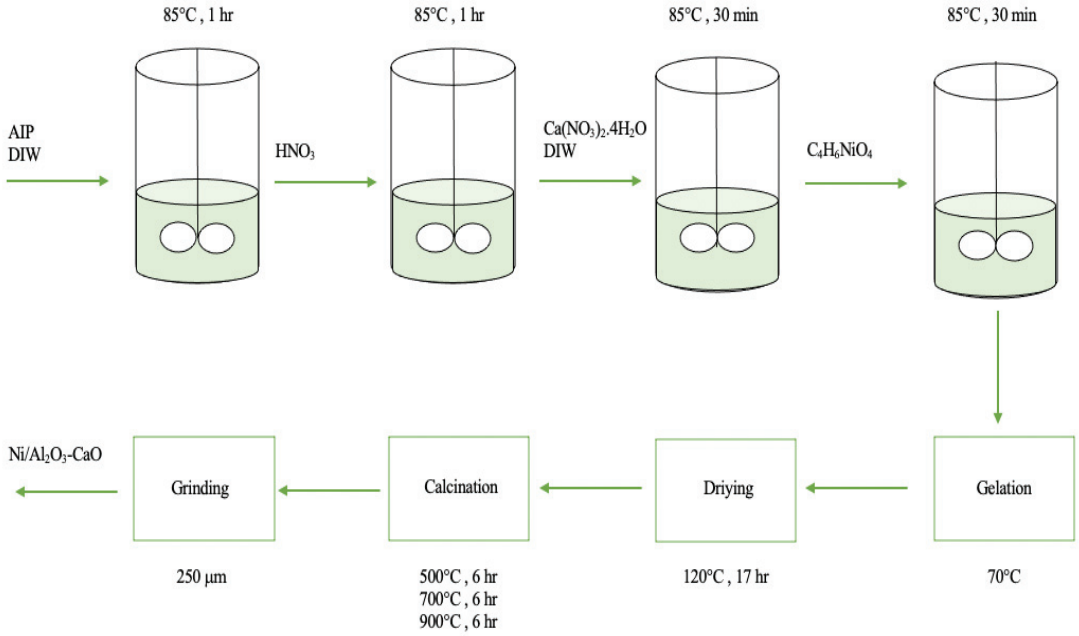

Figure 15. Experimental procedure for the preparation of Ni-Al_2O_3-CaO catalysts

After preparing alumina sol, calcium nitrate tetrahydrate as dissolved in half amount of deionized water used in sol preparation was added to the mixture at the same temperature. After 30 minutes, the certain amount of nickel acetate was added to the mixture. 30 minutes later, the temperature of mixture was decreased to 70°C and bottle cap was opened for letting evaporation of excess water to form nickel alumina calcium mix oxide gel. Afterwards, gel was dried at 120°C for 17 hours. Catalysts were calcinated at 500, 700 and 900°C for 6 hours with a heating rate of 10°C/min in air. At last, grinding step of all catalysts was carried out in a glove box by keeping humidity under 5%. 250 µm sieve was used. Ni-based catalysts were named as XNi-YAl-ZCa-T, where X, Y, Z

and T refer to nickel loading of the catalyst in wt.%, Al_2O_3 amount of support in wt.%, CaO amount of support in wt.% and calcination temperature in degree Celsius, respectively. Catalysts were denotated as 'fresh' before reaction and as 'spent' after used in 1 run of the reaction.

3.2.2. Catalytic Test

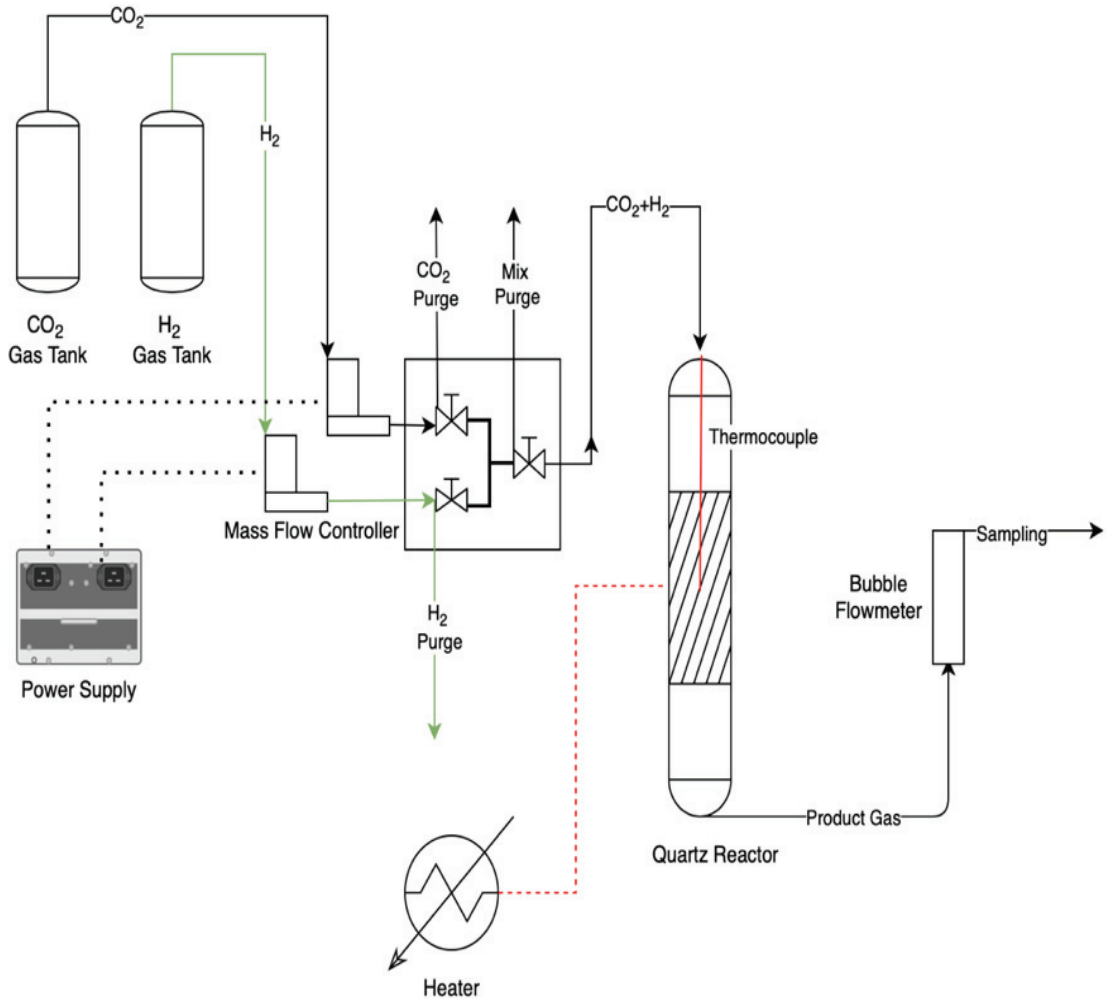

Figure 16. Description of Catalyst Testing Setup

Selected catalysts were tested and compared through CO_2 methanation reaction at reaction temperature of 400ºC with an inlet composition of CO_2/H_2 1/4 corresponding to flow rates of 20 mL/min and 80 mL/min without dilution gas. Reactions were carried out in a fixed bed continuous flow quartz reactor having an inner diameter of 4 mm. The reactor was fixed vertically inside a furnace and the temperature of reactor was controlled with a thermocouple inserted in the middle of the reactor tube. Before catalyst to be tested,

they were calcined again for 1 hour at the same calcination temperature in synthesis step with 50°C/min rate. Next, 100 mg of catalyst was placed into the reactor. Pure H_2 gas was fed into the system beginning from 150°C with a flow rate of 80 mL/min and heated to the reaction temperature. Then, the catalysts were pretreated for 20 minutes under H_2 gas at 400ºC. After the reduction treatment, the CO_2 stream was added to the system and the methanation reaction was started. Flow rate of product gas was monitored by a bubble flowmeter. After 45 minutes of reaction when the reaction was assumed to reach steady-state condition, the gaseous products generated from methanation were collected via a tedlar bag and analyzed with a GC-TCD.

3.2.3. Product Analysis

The reaction products analyzed with GC-TCD (Gas Chromatography –Thermal Conductivity Detector) with temperature programmed desorption technique to measure amount of CO_2 and methane in product gas. Perkin Elmer Clarus 500 Gas Chromatography was used for analysis. The CO_2 conversion, methane and CO selectivity, methane yield and carbon deposition were calculated by following equations.

$$X_{CO_2} = \frac{F_{CO_{2_{in}}} - F_{CO_{2_{out}}}}{F_{CO_{2_{in}}}}$$

$$S_i = \frac{F_i}{F_{CO_{2_{in}}} - F_{CO_{2_{out}}}}$$

$$Y_{CH_4} = \frac{F_{CH_{4_{out}}}}{F_{CO_{2_{in}}}}$$

$$Carbon\ Deposition = \frac{F_{CO_{2_{in}}} - (F_{CO_{2_{out}}} + F_{CH_{4_{out}}} + F_{CO_{out}})}{F_{CO_{2_{in}}}}$$

By utilizing the 10Ni-40Al-60Ca-700 catalyst five times, the experimental error was estimated. Same procedure was followed at those 5 experiments. Standard deviation (σ), uncertainty (U) and error were calculated by below given formulas at 95% confidence interval with t value of 2.776 for N is equal to 5.

$$\sigma = \sqrt{\frac{\Sigma\,(X - \overline{X})^2}{N}}$$

$$U = \frac{\sigma \times t_{N-1}}{\sqrt{N}}$$

$$error\% = \frac{U}{\overline{X}}$$

3.2.4. Catalyst Characterization

The crystalline phases of the selected fresh and spent catalysts were characterized by X-ray diffraction (XRD) on Philips X'Pert Pro X-ray diffractometer using Cu Kα radiation in the 2θ scanning range of 5-80° at 40 kV voltage, 40 mA current and a step size of 0.08°/s. Scherrer equation given below was used to calculate average crystalline sizes (d) of the catalysts.

$$\mathrm{d} = \frac{\mathrm{K} \times \lambda}{\beta \times \cos(\theta)}$$

where K is a constant of shape factor taking as 0.94, β is peak broadening effect using the full-width half maximum (FWHM) value in radians, θ is the main diffraction angle of the reflection in radian and λ, wavelength of X-ray, is 1.54056 Å which is characteristic to Cu Kα radiation.

Textural properties of the catalysts were determined based on Brunauer, Emmet and Teller (BET) method by N_2 adsorption isotherms at 77 K with volumetric adsorption device Micromeritics Gemini V. Just before the characterization, samples were calcined for degassing for 1 hour at their calcination temperature in the experimental part.

Spent catalysts were analyzed with a thermal gravimetric analyzer (Shimadzu TGA-51) to investigate carbon deposition behavior of catalysts with different formulations. Dry air was used as oxidizer to react with carbon deposit on the surface of the catalyst. Samples were heated up to their calcination temperatures with a heating rate of 10°C/min.

CHAPTER 4

RESULTS AND DISCUSSION

4.1. Thermodynamic Analysis of the Carbon Dioxide Methanation

Thermodynamic equilibrium calculations of chemical systems give information about the selectivity and yield of products, the effect of reaction parameters; temperature, pressure and reactant ratios. Comparing the thermodynamic analysis with experimental results makes possible to determine kinetic hindrances, i.e. thermodynamically allowed but in some way suppressed chemical reactions. Hence, thermodynamic calculations are helpful tools in catalyst development and process control of a particular reaction (Gao et al. 2012).

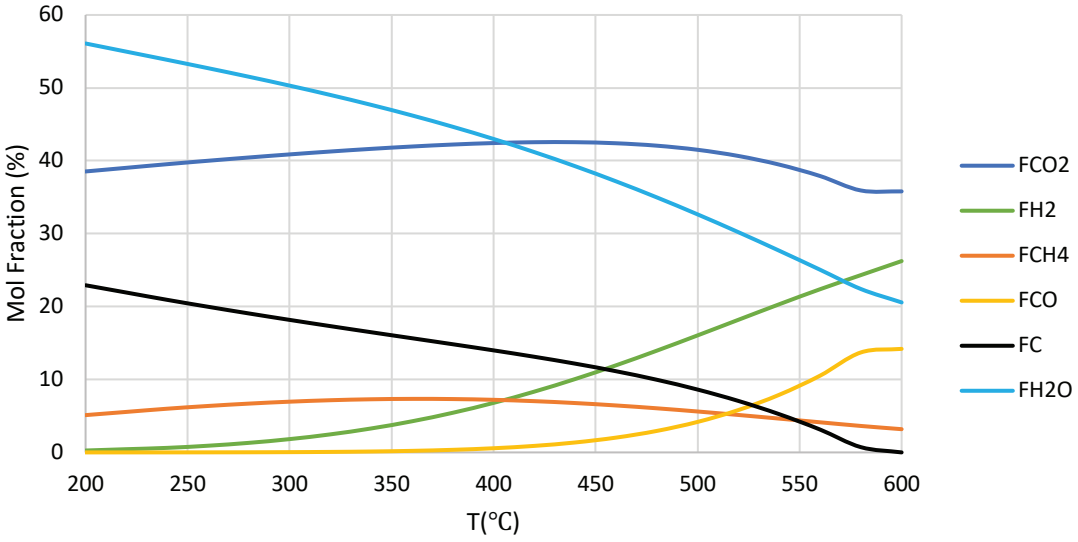

Figure 17. Effect of temperature on equilibrium compositions of CO_2 methanation for H_2/CO_2=1 at 1 atm

As evidenced by ΔH_{298K} value, the global reaction (reaction 1 in section 2.1) is highly exothermic such that the temperature rise for every 1% conversion can rise up to 61ºC in an adiabatic fixed-bed reactor (Wang, Zhen, and Yu 2016). According to Le

Chatelier's principle, low temperature and high pressure as being a volume-decreasing reaction favors the methanation of CO_2.

The number of independent reactions for carbon oxide methanation was found as 3 by matrix method. Reactions numbered 1, 4 and 6 in Table 2 were chosen as the set of independent reactions by considering the feed conditions (CO_2 and H_2) and all the involved species (CO_2, CO, H_2, CH_4, H_2O, C) are presented within these 3 reactions.

Table 2. Possible reactions involved in the methanation of carbon oxides (Source: Adapted from Mebrahtu; Krebs; Abate; Perathoner et al., 2019)

Reaction	**Reaction Type**	**ΔH_{298K} (kJ/mol)**
Methane Forming		
R1 $CO_{2(g)}+4H_{2(g)} \leftrightarrow CH_{4(g)}+2H_2O_{(g)}$	CO_2 methanation	-164.7
R2 $CO_{(g)}+3H_{2(g)} \leftrightarrow CH_{4(g)}+H_2O_{(g)}$	CO methanation	-205.9
R3 $2CO_{(g)}+2H_{2(g)} \leftrightarrow CH_{4(g)}+CO_{(g)}$	Inverse methane CO_2 reforming	-247.0
Shift Reaction		
R4 $CO_{2(g)}+H_{2(g)} \leftrightarrow CO_{(g)}+H_2O_{(g)}$	Reverse water-gas-shift (rWGS)	41.1
Carbon Forming		
R5 $2CO_{(g)} \leftrightarrow C_{(s)}+CO_{2(g)}$	Boudouard reaction	-172.4
R6 $CH_{4(g)} \leftrightarrow C_{(s)}+2H_{2(g)}$	Methane cracking	74.6
R7 $CO_{(g)}+H_{2(g)} \leftrightarrow C_{(s)}+H_2O_{(g)}$	CO reduction	-131.3
R8 $CO_{2(g)}+2H_{2(g)} \leftrightarrow C_{(s)}+2H_2O_{(g)}$	CO_2 reduction	-90.1

Figure 17 presents the thermodynamic equilibrium compositions of CO_2 methanation reaction for H_2/CO_2=1 feed condition. Since the feed conditions does not satisfy the stoichiometric ratio, CO_2 conversion and CH_4 selectivity cannot exceed 42% and 33%, respectively (Figure 18). Besides, considerable amount of carbon formation was observed which may lead carbon deposition and consequently catalyst deactivation.

In addition to this, Gao et al.'s study showed that when the H_2/CO_2 ratio is 2, CH_4 yield was as low as about 40% at 1 atm and 45% at 30 atm, respectively. Also abundant carbon deposition (up to 50%) was observed below 500ºC for both pressures indicating that in order to obtain a high CH_4 yield and avoid carbon deposition, H_2/CO_2 ratio should be equal or higher than the stoichiometric ratio of 4 (Gao et al. 2012).

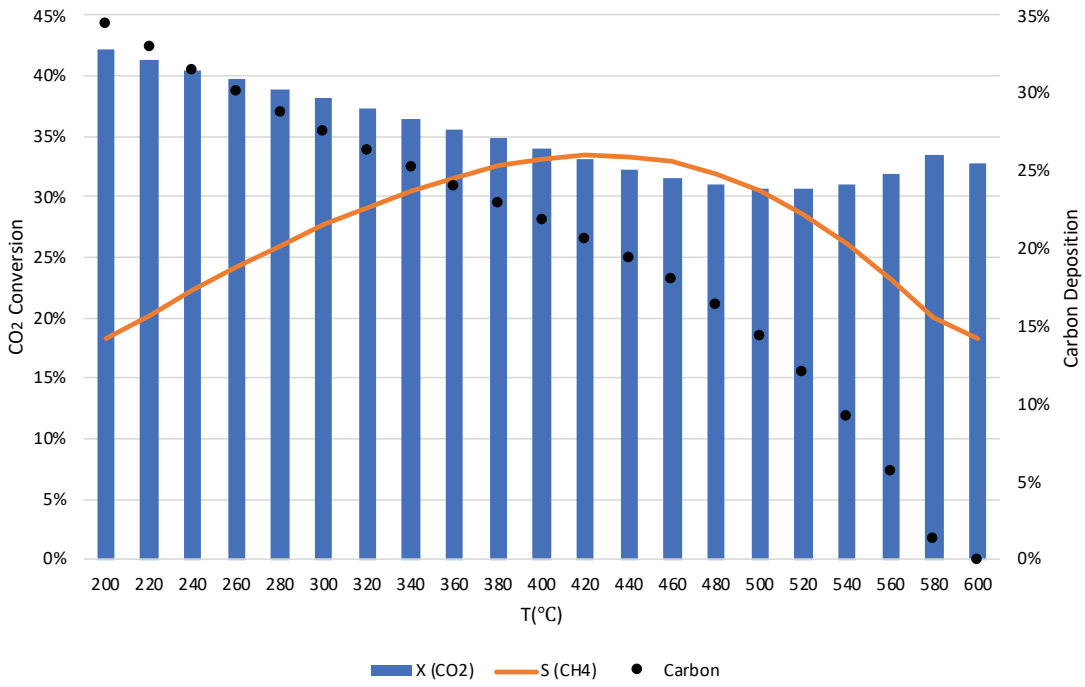

Figure 18. Effect of temperature on CO_2 conversion, CH_4 selectivity and Carbon formation for H_2/CO_2=1 at 1 atm

Effect of pressure was not investigated in here because catalyst evaluation of the CO_2 methanation is mostly conducted at atmospheric pressure. Besides, no significant change in methane yield between pressures 1 and 30 atm below 400 ºC was observed in the study of Gao et al.

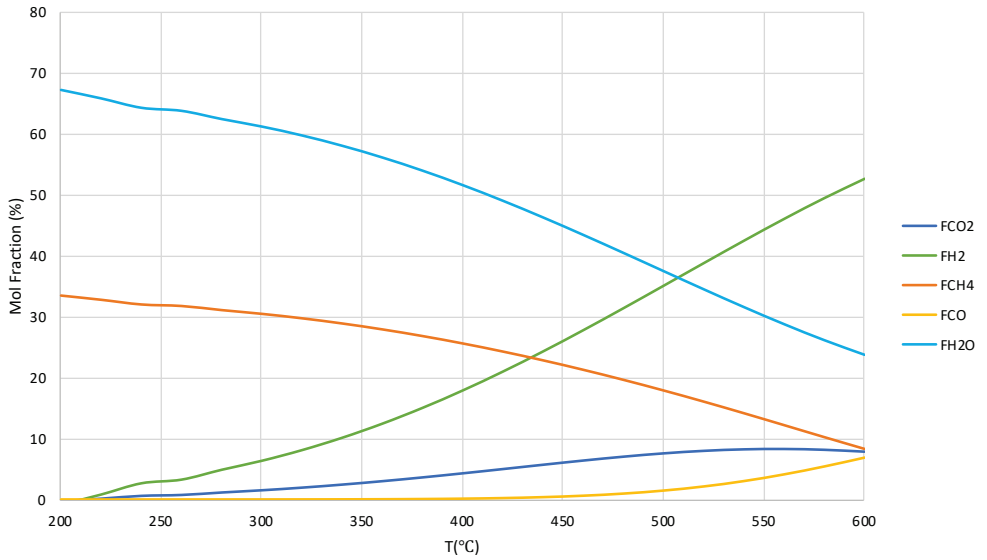

Figure 19. Effect of temperature on CO_2 methanation for H_2/CO_2=4 at 1 atm

Figure 19 presents the thermodynamic equilibrium compositions of CO_2 methanation reaction for H_2/CO_2=4 feed condition at 1 atm. At the stoichiometric ratio of reactants, carbon formation reaction (R6) does not take place and much higher CO_2 conversion and CH_4 selectivity can be reached (Figure 20). At ambient pressure, the temperature should not be higher than 360°C to maintain CO_2 conversion >90% and high selectivity to methane. Raising the reaction temperature above 450ºC resulted in increase of carbon monoxide by-product due to the reverse water–gas shift reaction, and meanwhile, unreacted carbon dioxide and hydrogen also increased, along with a significant decrease in the methane yield.

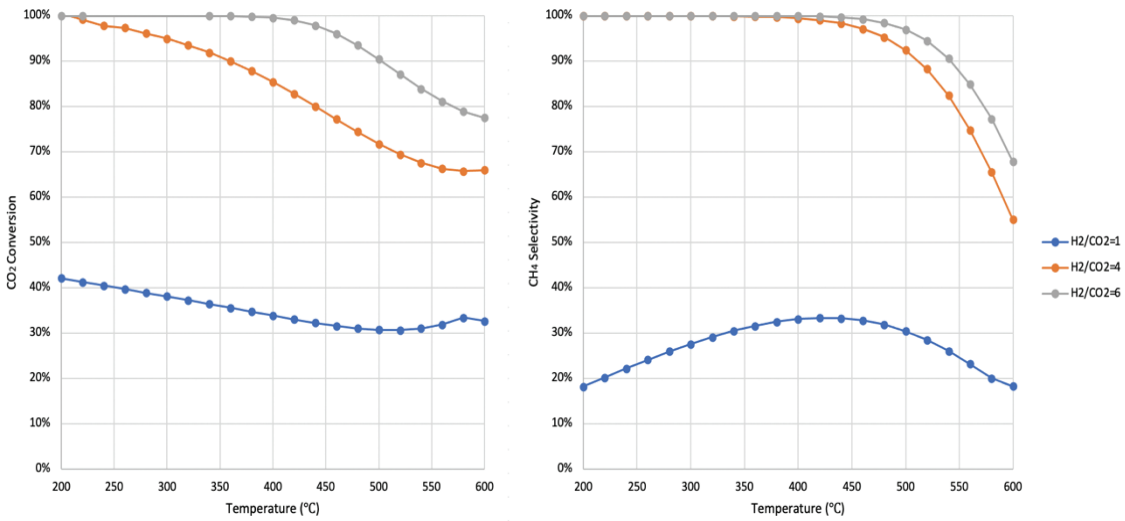

Figure 20. Effect of temperature and H_2/CO_2 ratio on CO_2 methanation at 1 atm

CO_2 conversion and methane selectivity can be further enhanced by increasing H_2/CO_2 ratio from 4 to 6 at the same pressure as can be seen from Figure 20. At this feed ratio, temperature sensitivity of the reaction was minimized due to excess amount of H_2. Although $H_2/CO_2>4$ seems to be beneficial due to high methane yields and elimination of carbon formation, considerable amount of valuable green hydrogen is left in the product gas and regulations only allow a few percentages of hydrogen content in SNG to be fed to gas grids (Mebrahtu et al. 2019). Thereby, reaction conditions were chosen as stoichiometric ratio of reactants, 400 ºC and 1 atm. Equilibrium data based on the Ideal Gas assumption at these conditions were given in Table 3.

Table 3. Equilibrium calculation of CO_2 methanation (H_2/CO_2=4, 400 ºC, 1 atm)

X CO_2	**S CH_4**	**S CO**	**Y CH_4**
0.855	0.995	0.005	0.850

According to thermodynamic analysis, CO_2 methanation can reach 100% methane selectivity in particular at low temperatures. Theoretically, it means elimination of subsequent product separation. Such a thermodynamic feature makes Sabatier reaction one of the most advantageous way of storing renewable energy and handling CO_2 emissions in terms of energy efficiency and economic feasibility. However, this is not practical, because the reaction is limited by kinetics. This kinetic barrier can be overcome through the use of an appropriate catalyst; hence carbon dioxide can be methaneted under mild conditions (low temperature and atmospheric pressure) with high CH_4 yields.

4.2. Crystalline Phases of the Catalysts

In order to understand the reasons for varied conversions on the catalysts prepared with different compositions and calcination temperature, the crystalline phases and their average sizes of the catalysts were determined by means of XRD. The crystalline phases in the fresh and spent catalysts were identified by using X'Pert Highscore Plus Programme. The XRD patterns of fresh catalysts calcined at 700°C with varied calcium content were displayed in Figure 21. The average crystallite sizes of the phases were calculated via Scherrer equation and listed in Table 4.

Diffraction peaks at 2θ of 37.2°, 43.3°, 62.9° corresponding NiO species were observed in Ca doped catalysts except from 10Ni-70Al-30Ca-700 where NiO particles might be highly dispersed on surface of $70Al_2O_3$-30CaO support. Moreover, the peak intensities belonging only NiO phase remained unaffected when Ca amount increased, which indicates that dispersion of NiO species did not change by CaO addition. On unmodified catalyst (without calcium), there was a different Ni phase assigned to $NiAl_2O_4$ corresponding to peaks located at 37.01°, 44.99° and 65.54°. $NiAl_2O_4$ peaks were very broad, as an indication of very small crystal size (<5nm).

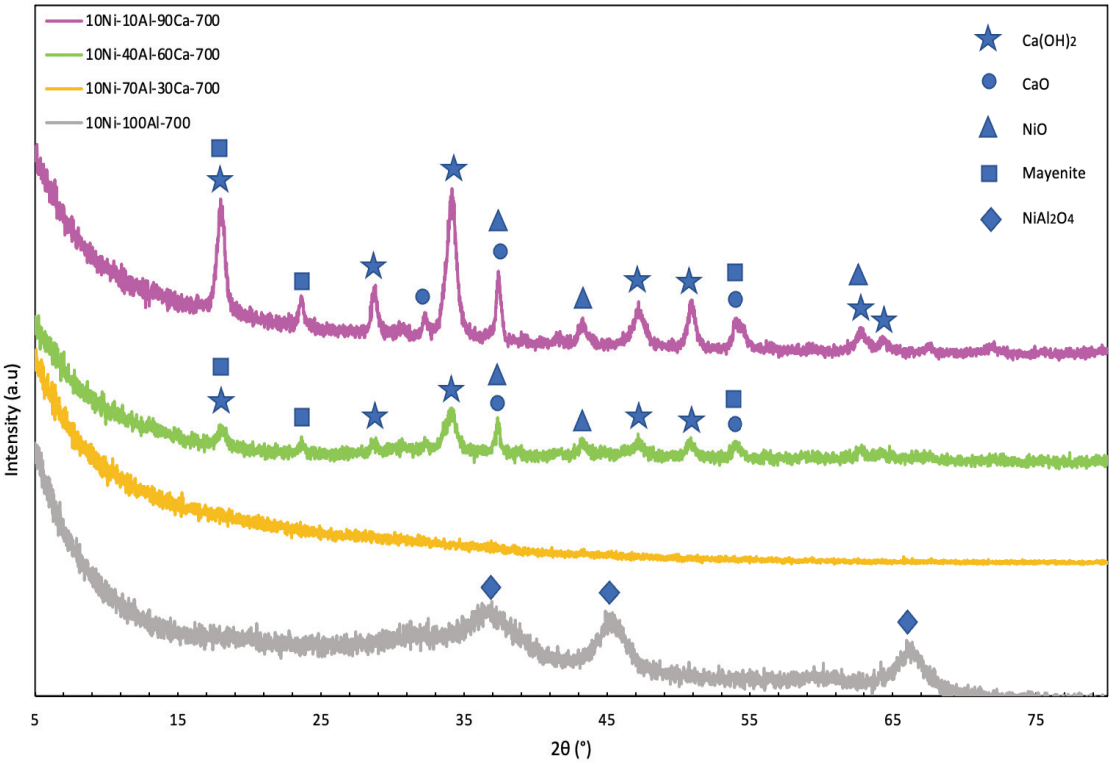

Figure 21. X-Ray Diffraction spectra of fresh catalysts

Calcium was present in the form of $Ca(OH)_2$, CaO, mayenite ($Ca_{12}Al_{l4}O_{33}$) for catalysts supported on $40Al_2O_3$-60CaO and $10Al_2O_3$-90CaO but again no clear diffraction peaks of calcium derived species were detected for $70Al_2O_3$-30CaO, indicating that Ca may have formed amorphous phases or was below the detection limit of XRD. In other words, calcium and alumina might be well incorporated, so the growth of crystallites greater than 5 nm was prevented. In $40Al_2O_3$-60CaO and $10Al_2O_3$-90CaO catalysts' structure, the presence of mayenite species ($Ca_{12}Al_{l4}O_{33}$) could also imply that calcium was successfully incorporated in aluminum matrix due to modified sol-gel

method. From Table 4, it was seen that NiO crystallite sizes were not significantly affected by increasing calcium amount whereas CaO and mayenite crystallite sizes underwent severe changes.

Table 4. Crystalline phases and crystallite sizes (nm) of fresh catalysts

Catalysts ID	$Ca(OH)_2$	CaO	NiO	Mayenite	$NiAl_2O_4$
10Ni-10Al-90Ca-700	16.71	28.67	16.37	26.29	-
10Ni-40Al-60Ca-700	15.83	18.29	17.07	19.74	-
10Ni-70Al-30Ca-700	-	-	-	-	-
10Ni-100Al-700	-	-	-	-	<5

The interaction strength of CaO and aluminum among catalysts calcined at 700°C might lead to agglomeration of Ca particles with increasing calcium content, resulting in rising crystallite sizes of CaO and mayenite species in between 10Ni-40Al-60Ca-700 and 10Ni-10Al-90Ca-700. On the other hand, calcium hydroxide $Ca(OH)_2$, which is derived from CaO and water, did not exhibit any significant growth when calcium levels increased.

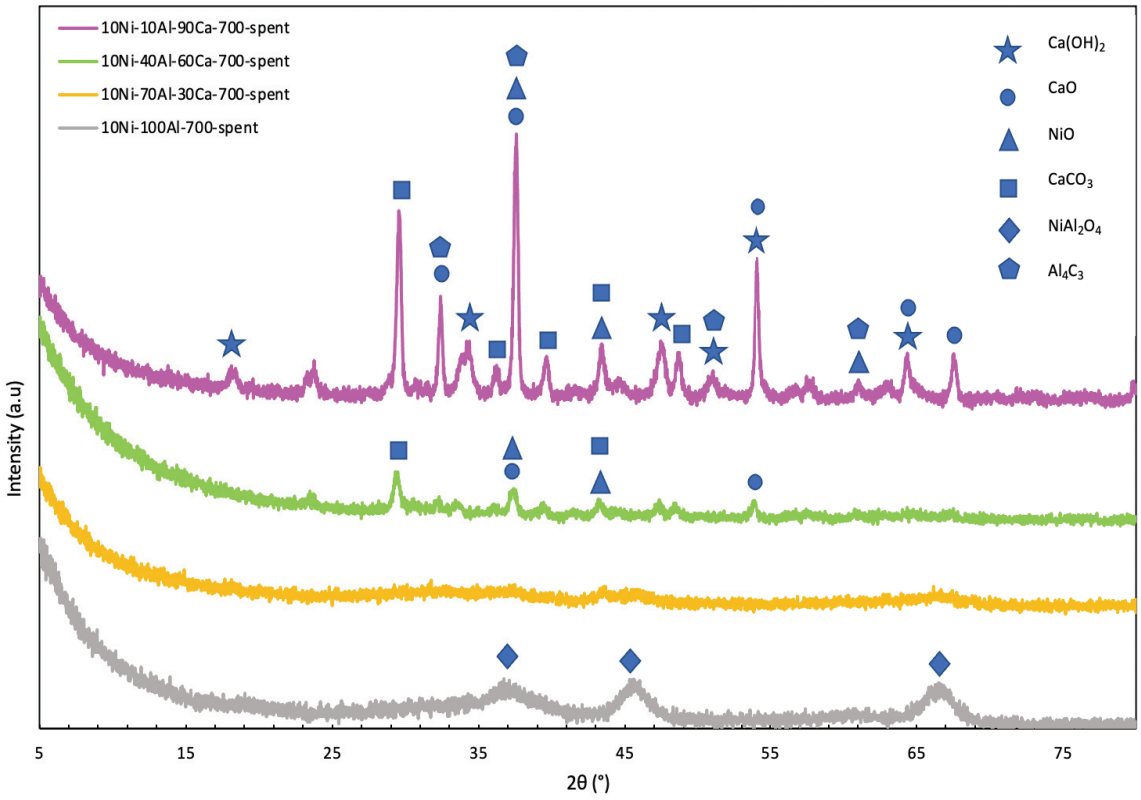

Figure 22. X-Ray Diffraction spectra of spent catalysts

The XRD patterns of spent catalysts calcined at 700°C with varied calcium content were displayed in Figure 22 and the average crystallite sizes of the phases were listed in Table 5. After employed in the reaction, while mayenite species were disappeared, calcite ($CaCO_3$) phase was appeared in 10Ni-10Al-90Ca-700 and 10Ni-40Al-60Ca-700 catalysts corresponding to main peaks located at 29.47°, 43.25°, 47.22° which has a higher average crystallite size for former. Calcium hydroxide and carbon dioxide combine to form the calcite phase. As a result, it was assumed that this was the cause of the decline and disappearance of $Ca(OH)_2$ crystals.

Additionally, over spent 10Ni-10Al-90Ca-700, aluminum carbide (Al_4C_3) was observed to form indicating formation of carbonous species during methanation reaction.

Table 5. Crystalline phases and crystallite sizes (nm) of spent catalysts

Catalysts ID	$Ca(OH)_2$	CaO	$CaCO_3$	NiO	Al_4C_3	$NiAl_2O_4$
10Ni-10Al-90Ca-700	10.83	28.99	22.85	12.59	*	-
10Ni-40Al-60Ca-700	-	10.83	19.91	*	-	-
10Ni-70Al-30Ca-700	-	-	-	<5	-	-
10Ni-100Al-700	-	-	-	-	-	<5

***: could not be calculated**

4.3. Textural Properties of the Catalysts

N_2 adsorption-desorption isotherms of the fresh 10Ni-10Al-90Ca-700 and 10Ni-100Al-700 was shown in Figure 23. It could be observed that both samples exhibited IV type curve with hysteresis loops. This implied mesoporous solids with capillary condensation (Xu et al. 2017).

Table 6. Textural properties of catalysts with and without CaO

Catalysts ID	Specific Surface Area [a] (m^2/g)	Pore Volume [b] ($x10^{-2}$ cm^3/g)	Pore Diameter [c] (nm)
10Ni-10Al-90Ca-700	17.4859	2.76	3.97
10Ni-100Al-700	171.1088	28.54	4.47

[a]: evaluated based on Brunauer-Emmett-Teller theory

[b]:calculated based on Barrett-Joyner-Halenda (BJH) theory

[c]:BJH desorption average pore diameter

The BET specific surface area, pore volume and pore diameter of modified and unmodified catalysts calcined at 700°C were presented in Table 6. It can be seen that the

addition of CaO resulted in almost 10-fold decrease in surface area and pore volume of the catalysts due to blockage of some part of mesopores. While modified catalyst suffers from low surface area (~17.49 m^2/g), higher surface area of unmodified catalysts (~171.11 m^2/g) suggests better dispersion of components which was evidenced by very small crystal size of $NiAl_2O_4$. In addition, it was notable that the samples modified with Ca displayed slightly smaller pore diameter than pristine Ni/Al_2O_3 catalyst. Smaller pore diameter suggested that calcium nanoparticles could regulate pore diameter by taking part in the synthesis process. The change in NiO and Al_2O_3 structures through their interaction with CaO might be responsible for the change in textural properties.

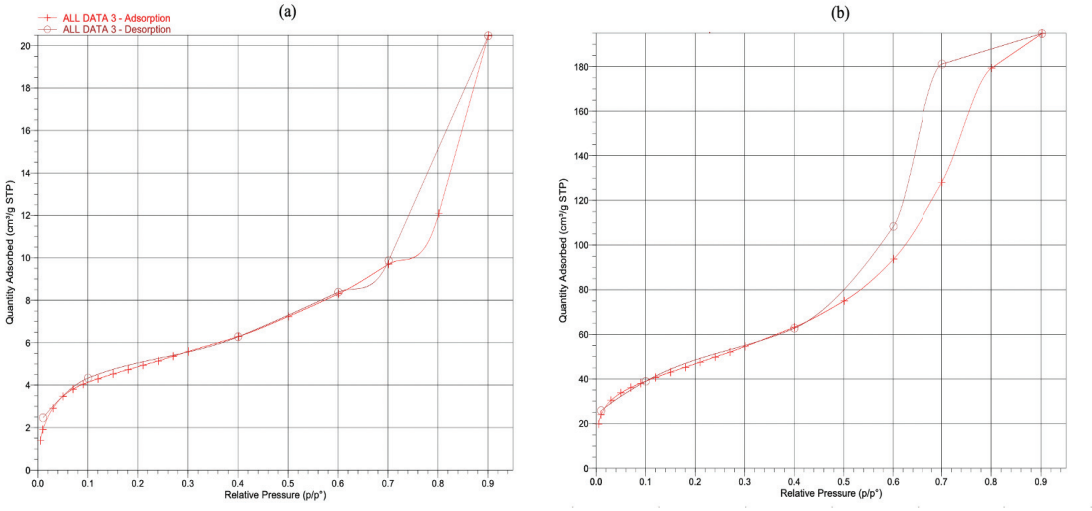

Figure 23. Nitrogen adsorption-desorption isotherms; a)10Ni-10Al-90Ca-700 b)10Ni-100Al-700

4.4. Catalyst Activity

Firstly, the influence of Ni loading on catalytic activity was investigated over Ni catalysts supported on $70Al_2O_3$-30CaO and calcined at 500°C, 700°C, 900°C. As can be seen from Table 7, regardless of calcination temperature, 1 wt.% loaded Ni-70Al-30Ca catalysts produced no methane and increasing Ni loading resulted in increased CO_2 conversion and methane selectivity. This increment was more pronounced for catalysts calcined at 700ºC with methane yields of 0%, 6.72% and 28.79% for 1, 5 and 10 wt.% Ni loadings, respectively.

CO_2 conversion, methane selectivity, yield and carbon deposition over 700ºC calcined catalysts were represented as a function of Ni content in Figure 24. While a large extent of carbon dioxide converted into carbon deposit on 5 wt.% nickel loaded catalyst, 10Ni-70Al-30Ca-700 catalyst showed the highest selectivity toward methane but also CO, indicating CO_2 activation energy was lowered. Over 1 wt.% Ni loaded catalyst, neither CO_2 nor H_2 were activated. As evidenced by XRD patterns, outperformance of 10Ni-70Al-30Ca-700 catalyst may be due to the high dispersion of NiO particles. Therefore, it is conceivable that the alumina-calcium mixed oxide support could disperse higher loadings of Ni, which could result in higher CO_2 conversion.

However, 1 and 5 wt.% Ni loaded 70Al-30Ca-700 catalysts also showed no clear diffraction peaks in XRD as given in Appendix A. Those low Ni loaded catalysts were expected to have smaller Ni particle sizes than 10Ni-70Al-30Ca-700 catalyst, but the number of active sites were not sufficient for dissociative adsorption of reactants. As a result, the number of Ni active sites was found to have a significant impact on CO_2 methanation.

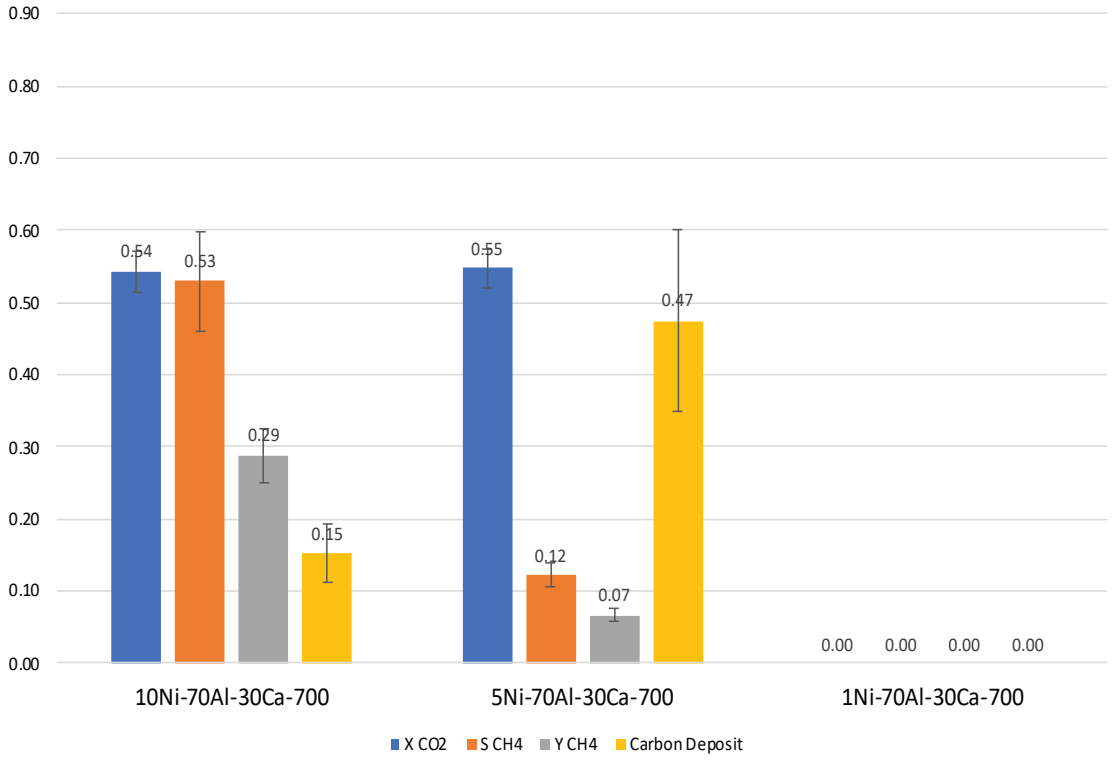

Figure 24. Effect of Ni loading on catalytic performance

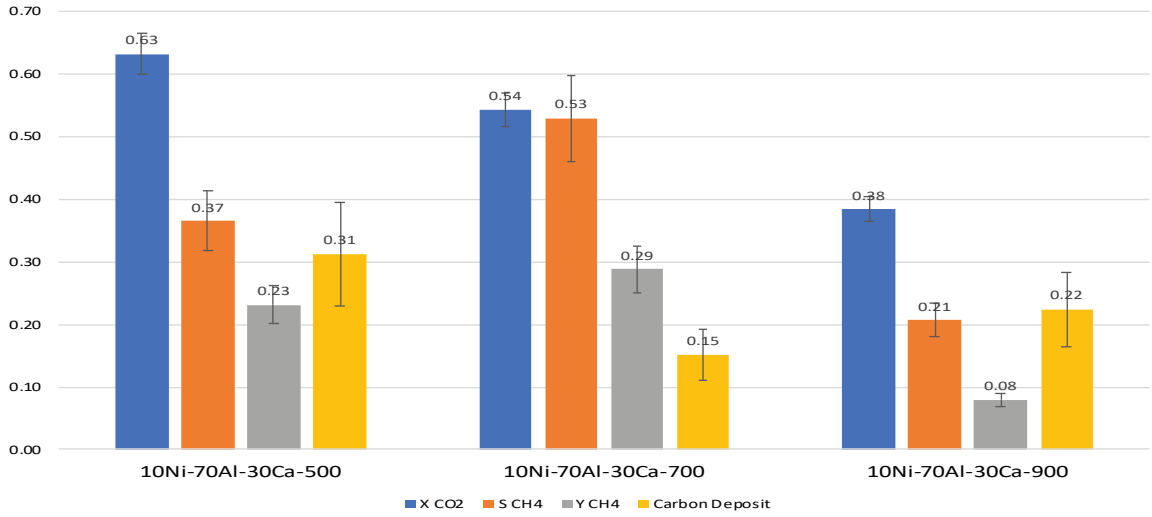

Figure 25. Effect of calcination temperature on catalytic performance

In order to understand the effect of calcination temperature, 10 wt.% Ni loaded catalysts were chosen as the basis of comparison due to higher CO_2 conversion obtained in the previous section. Results were demonstrated in Figure 25. With the same catalyst formula, catalysts calcined at 900ºC showed poorer catalytic activity towards methanation than 500ºC and 700ºC calcined fellows. Over the catalysts calcined at the temperature of 900ºC, maximum methane yield was obtained over 10Ni-70Al-30Ca-900 as 8%. During the calcination process at 900ºC, the structure of the catalyst might be damaged. As a result of the thermal shrinkage of the structure, the pore size of the catalyst decreases when the calcination temperature rises. Increasing calcination temperature from 700°C to 900°C caused a significant decrease in methane yield that might be due to lowering surface area to disperse Ni species. While, highest CO_2 conversion was obtained among 10 wt.% nickel supported on $70Al_2O_3$-30CaO catalyst with 500ºC calcination temperature, highest methane selectivity achieved by catalyst calcined at 700ºC. When the experimental error margins (Table 8) are included, it may be concluded that they performed similarly.

Table 7. Reproducibility of the experiments

	%Error
X CO_2	10.22
S CH_4	25.93
Y CH_4	26.36
S CO	8.15
Carbon Deposition	53.18

Table 8. CO_2 conversion, methane selectivity and yield, carbon deposition in catalytic experiments

$T_{cal.}$	Catalyst ID	X CO_2	S CH_4	Y CH_4	S CO	Carbon Deposition
500°C	10Ni-70Al-30Ca-500	0.63	0.37	0.23	0.14	0.31
	5Ni-70Al-30Ca-500	0.22	0.32	0.07	0.37	0.07
	1Ni-70Al-30Ca-500	0.05	0.00	0.00	0.03	0.05
700°C	10Ni-10Al-90Ca-700	0.76	0.79	0.60	0.04	0.13
	10Ni-40Al-60Ca-700	0.24	0.45	0.11	0.30	0.06
	10Ni-70Al-30Ca-700	0.54	0.53	0.29	0.19	0.15
	10Ni-100Al-700	0.38	0.00	0.00	0.01	0.37
	5Ni-70Al-30Ca-700	0.55	0.12	0.07	0.01	0.47
	1Ni-70Al-30Ca-700	0.00	0.00	0.00	0.00	0.00
900°C	10Ni-70Al-30Ca-900	0.38	0.21	0.08	0.21	0.22
	5Ni-70Al-30Ca-900	0.14	0.11	0.01	0.36	0.07
	1Ni-70Al-30Ca-900	0.07	0.00	0.00	0.00	0.07

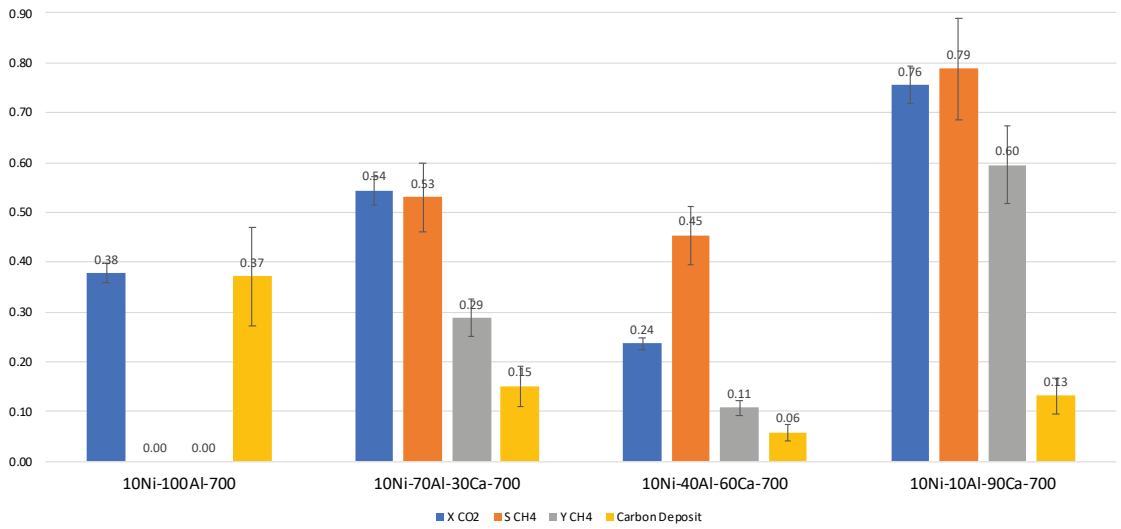

Figure 26. Effect of calcium content on catalytic performance

Lastly, the Ni/Al_2O_3 reference catalyst and modified catalysts with different amount of CaO were applied for methanation of CO_2. In Figure 26, CO_2 conversion, methane selectivity and yield as well as carbon deposition were compared as a function of catalyst composition. The reference catalyst has shown no activity towards CO_2

methanation at the reaction conditions applied. This could be mainly attributed to $NiAl_2O_4$ phase presents as the only Ni specie in the structure of the catalyst. It was consistent with the literature; increase in the proportion of inactive $NiAl_2O_4$ phase caused a significant decrease in CO_2 conversion (Rahmani, Rezaei, and Meshkani 2014). It was obvious that Ca modification had a significant impact on methane production. The promotion of catalytic performance may arise from intensifying the CO_2 chemisorption by introducing basic modifier. CaO was reported to increase number as well as the intensity of basic sites over the catalysts that decreases the activation energy of CO_2 (Lv et al. 2020).

CO_2 conversion and methane selectivity over modified catalysts first decreased and then increased, attaining the highest value with 10Ni-10Al-90Ca-700 among all the catalyst listed in Table 7. When calcium level increased from 30 wt.% to 60 wt.%, methane yield declined from 29% to 11% because of increased selectivity to CO by-product. Lower CO_2 conversion of 10Ni-40Al-60Ca-700 among modified catalysts in Figure 26, was attributed to absence of calcium hydroxide species in spent catalyst. It was likely to all calcium hydroxide species on the surface combined with CO_2, resulting in slow CO_2 dissociation. It was widely believed that CO_2 adsorption and dissociation are the first step in mechanism of CO_2 methanation and CO_2 dissociation into CO through rWGS is suggested as having competitive effect to hydrogen adsorption. When the calcium content was 30 wt.%, it was assumed that there were a limited number of basic sites for CO_2 adsorption, so CO_2 and H_2 adsorbed and dissociated primarily on the same part of the catalyst (Ni particles), resulting in less selective methanation when compared to the 10Ni-10Al-90Ca-700 catalyst. With calcium levels of 60 wt.% and 90 wt.%, calcite species were detected in XRD spectra of the spent catalysts and they were generated by combination of calcium hydroxide and carbon dioxide, implying that CO_2 adsorbed on basic support rather than active component.

4.5. Carbon Deposition Analysis of Catalysts

Previous research has demonstrated that weight loss in the Thermogravimetric analysis (TGA) characterization of the catalyst after the methanation reaction is primarily due to carbon deposition oxidation. Since carbon formation may lead catalyst deactivation by blocking the pores and decreasing the metal surface area, further

investigation on the carbon deposition behavior of the catalyst was conducted. Carbon deposition over the fresh and spent 10Ni-10Al-90Ca-700 catalyst were illustrated in Figure 27. The color of the catalyst darkened noticeably after 45 minutes of reaction. In the same manner, Table 9 displays carbon deposition behavior over the reaction time.

Table 9. Effect of reaction time over 10Ni-10Al-90Ca-700 catalyst

Reaction Time	X CO_2	S CH_4	Y CH_4	S CO	Carbon Deposition
10 min.	0.84	0.58	0.49	0.02	0.34
45 min	0.76	0.79	0.60	0.04	0.13

The results of experiment with 10Ni-10Al-90Ca-700 catalyst showed that CO_2 conversion almost approached to equilibrium conversion, yet selectivity was far from thermodynamic calculations. As the reaction progresses, the amount of carbon deposition was observed to decrease. While consumption of CO_2 remained constant within the experimental error, methane selectivity increased. Inlet and outlet molar flow rates of components in two experiments with 10Ni-10Al-90Ca-700 catalyst were given in Appendix B.

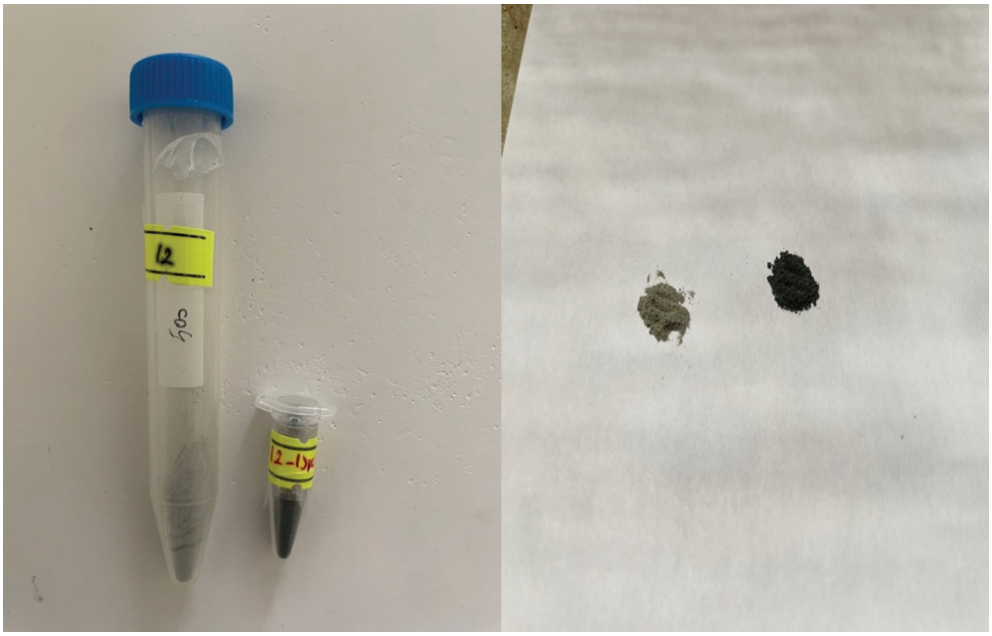

Figure 27. 10Ni-10Al-90Ca-700 catalyst before and after the reaction

In Figure 28, TGA results of spent catalysts with varying Ca content were given. According to the figure, reference catalyst without Ca addition subjected to the highest weight loss of 12.74% occurring at 101.6ºC due to vaporization of water. Catalysts with

30 wt.%, 60 wt.% and 90 wt.% CaO addition showed 6.87%, 2.09% and 7.05% weight loss, respectively. Whereas spent 10Ni-70Al-30Ca-700 catalyst showed one weight reduction centered at 112.6ºC, two separate weight reductions at 477.2ºC and 650.2ºC were observed for spent 10Ni-10Al-90Ca-700 catalyst, with the former being more noticeable. Thermogravimetric research and XRD results showed that increasing calcium level to 90 wt.% could result in formation of carbonous species, aluminum carbide (Al_4C_3), which were oxidized at 650ºC. The distinctive weight loss of 10Ni-10Al-90Ca-700 at 477.2ºC was attributed to water and CO_2 desorption which could be the reason of the most selective CO_2 methanation among the tested catalysts. During methanation, a calcium content of 90% seem to be intensified CO_2 chemisorption and activation.

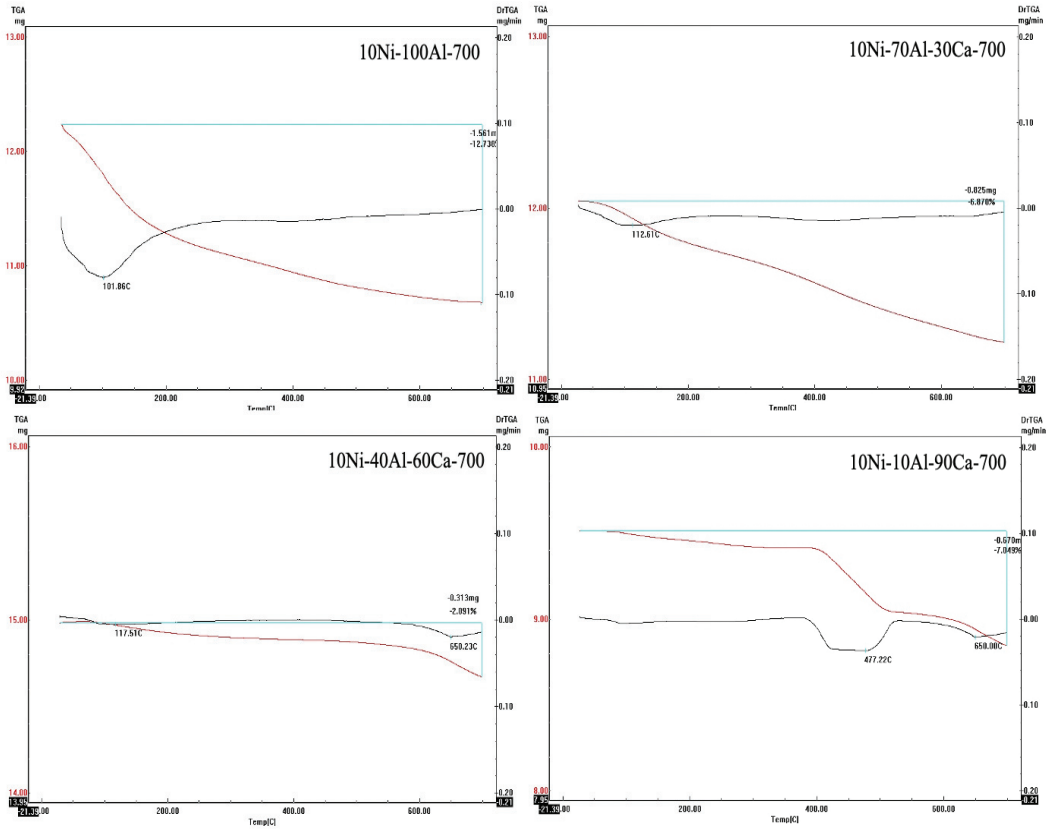

Figure 28. Thermogravimetric analysis of spent catalysts

CHAPTER 5

CONCLUSION

Under the PtG technology, catalytic conversion of CO_2 to produce methane, renewable natural gas, is considered as one of the most efficient and convenient strategy for not only reducing CO_2 emissions but also storing surplus renewable energy in chemical media. Despite the fact that precious metals have greater low-temperature catalytic activity and stability in CO_2 methanation, Ni-based catalysts with superior low-temperature catalytic performance are a hot research topic due to their lower cost and availability. It is, however, well-known that Ni catalysts suffer from its short lifetime because of carbon deposition.

The study attempts to understand the effect of support basicity on Sabatier reaction and improve the performance of Ni based catalysts by introducing calcium which is known for its basicity. In accordance with this purpose, 1,5 and 10 wt.% Ni loaded-Al_2O_3-CaO mix oxide catalysts were synthesized with modified sol-gel method and calcinated at the temperatures of 500ºC, 700ºC and 900ºC for 6 hours. Al_2O_3-CaO supports were synthesized at three ratios as follows; 70-30 wt.%, 40-60 wt.%, 10-90 wt.% wherein Ni/Al_2O_3 catalyst was used as reference catalyst. Based on thermodynamic analysis, reaction was conducted at 400ºC and 1 atm with inlet composition of CO_2/H_2=1/4 and total volumetric flow rate of 100 ml/min.

Reference catalyst calcined at 700ºC were found to be inactive at used reaction conditions due to the presence of inactive $NiAl_2O_4$ phase. With the same catalyst formula, catalysts calcined at 900ºC showed poorer catalytic activity towards methanation than 500ºC and 700ºC calcined fellows. Increasing Ni loading increased both CO_2 conversion and methane selectivity. The influence of Ni loading was more pronounced for catalysts calcined at 700ºC. Ca modification was found to have a prominent impact on methane yield. With 10Ni-10Al-90Ca-700, being best performing catalyst, CO_2 conversion obtained as 76% and methane yield was 60%. The promotion of catalytic performance may arise from intensifying the CO_2 chemisorption confirmed by XRD and TGA results.

REFERENCES

Aldana, P. A. U., F. Ocampo, K. Kobl, B. Louis, F. Thibault-Starzyk, M. Daturi, P. Bazin, S. Thomas, and A. C. Roger. 2013. "Catalytic CO2 valorization into CH4 on Ni-based ceria-zirconia. Reaction mechanism by operando IR spectroscopy." *Catalysis Today* 215: 201-207.

Ari, Izzet, and Riza Fikret Yikmaz. 2019. "The role of renewable energy in achieving Turkey's INDC." *Renewable and Sustainable Energy Reviews* 105: 244-251.

E. Dace, J. Rusanova, J. Gusca, and D. Blumberga. 2014. "Selecting a catalyst for methanation process: Technical and economic performance based TOPSIS analysis." *Proceedings of the 27th International Conference on Efficiency, Cost, Optimization, Simulation and Environmental Impact of Energy Systems, Scopus Finland*

Gao, J. J., Q. Liu, F. N. Gu, B. Liu, Z. Y. Zhong, and F. B. Su. 2015. "Recent advances in methanation catalysts for the production of synthetic natural gas." *Rsc Advances* 5 (29): 22759-22776.

Gao, J. J., Y. L. Wang, Y. Ping, D. C. Hu, G. W. Xu, F. N. Gu, and F. B. Su. 2012. "A thermodynamic analysis of methanation reactions of carbon oxides for the production of synthetic natural gas." *Rsc Advances* 2 (6): 2358-2368.

Garbarino, G., P. Riani, L. Magistri, and G. Busca. 2014. "A study of the methanation of carbon dioxide on Ni/Al2O3 catalysts at atmospheric pressure." *International Journal of Hydrogen Energy* 39 (22): 11557-11565.

Graca, I., L. V. Gonzalez, M. C. Bacariza, A. Fernandes, C. Henriques, J. M. Lopes, and M. F. Ribeiro. 2014. "CO2 hydrogenation into CH4 on NiHNaUSY zeolites." *Applied Catalysis B-Environmental* 147: 101-110.

Hutchings, G. J., & Védrine, J. C. (2004). Heterogeneous catalyst preparation. In *Basic principles in applied catalysis* (pp. 215-258). Springer, Berlin, Heidelberg.

Kırlı, Mustafa Safa, and Murat Fahrioğlu. 2018. "Sustainable development of Turkey: Deployment of geothermal resources for carbon capture, utilization, and storage."

Energy Sources, Part A: Recovery, Utilization, and Environmental Effects 41 (14): 1739-1751.

Lee, Woo Jin, Chaoen Li, Hermawan Prajitno, Jiho Yoo, Jim Patel, Yunxia Yang, and Seng Lim. 2021. "Recent trend in thermal catalytic low temperature CO2 methanation: A critical review." *Catalysis Today* 368: 2-19.

Li, Wenhui, Haozhi Wang, Xiao Jiang, Jie Zhu, Zhongmin Liu, Xinwen Guo, and Chunshan Song. 2018. "A short review of recent advances in CO2 hydrogenation to hydrocarbons over heterogeneous catalysts." *RSC Advances* 8 (14): 7651-7669.

Lv, C., L. Xu, M. Chen, Y. Cui, X. Wen, Y. Li, C. E. Wu, B. Yang, Z. Miao, X. Hu, and Q. Shou. 2020a. Recent Progresses in Constructing the Highly Efficient Ni Based Catalysts With Advanced Low-Temperature Activity Toward CO2 Methanation. Front Chem.

---. 2020b. "Recent Progresses in Constructing the Highly Efficient Ni Based Catalysts With Advanced Low-Temperature Activity Toward CO2 Methanation." *Front Chem* 8: 269.

M. A. A. Aziz, A. A. Jalil, S. Triwahyono,A. Ahmad. 2015. "CO2 methanation over heterogeneous catalysts: recent progress and future prospects." *Green Chemistry* 17 (5): 2647-2663.

Martin, N. M., P. Velin, M. Skoglundh, M. Bauer, and P. A. Carlsson. 2017. "Catalytic hydrogenation of CO2 to methane over supported Pd, Rh and Ni catalysts." *Catalysis Science & Technology* 7 (5): 1086-1094.

Mebrahtu, Chalachew, Florian Krebs, Salvatore Abate, Siglinda Perathoner, Gabriele Centi, and Regina Palkovits. 2019. "CO2 Methanation: Principles and Challenges." In *Horizons in Sustainable Industrial Chemistry and Catalysis*, In Studies in Surface Science and Catalysis, 85-103.

Miao, Bin, Su Su Khine Ma, Xin Wang, Haibin Su, and Siew Hwa Chan. 2016. "Catalysis mechanisms of CO2 and CO methanation." *Catalysis Science & Technology* 6 (12): 4048-4058.

Muller, K., M. Stadter, F. Rachow, D. Hoffmannbeck, and D. Schmeisser. 2013. "Sabatier-based CO2-methanation by catalytic conversion." *Environmental Earth Sciences* 70 (8): 3771-3778.

Ocampo, Fabien, Benoit Louis, and Anne-Cécile Roger. 2009. "Methanation of carbon dioxide over nickel-based Ce0.72Zr0.28O2 mixed oxide catalysts prepared by sol–gel method." *Applied Catalysis A: General* 369 (1): 90-96.

Owusu, Phebe Asantewaa, Samuel Asumadu-Sarkodie, and Shashi Dubey. 2016. "A review of renewable energy sources, sustainability issues and climate change mitigation." *Cogent Engineering* 3 (1).

Pan, Yun-xiang, Chang-jun Liu, and Qingfeng Ge. 2010. "Effect of surface hydroxyls on selective CO2 hydrogenation over Ni4/γ-Al2O3: A density functional theory study." *Journal of Catalysis* 272 (2): 227-234.

Rafiee, Ahmad, Kaveh Rajab Khalilpour, and Dia Milani. 2019. "CO2 Conversion and Utilization Pathways." In *Polygeneration with Polystorage for Chemical and Energy Hubs*, 213-245.

Rahmani, Soudabeh, Mehran Rezaei, and Fereshteh Meshkani. 2014. "Preparation of highly active nickel catalysts supported on mesoporous nanocrystalline γ-Al2O3 for CO2 methanation." *Journal of Industrial and Engineering Chemistry* 20 (4): 1346-1352.

Richardson, James T. 2013. *Principles of catalyst development*. Springer.

Rönsch, Stefan, Jens Schneider, Steffi Matthischke, Michael Schlüter, Manuel Götz, Jonathan Lefebvre, Praseeth Prabhakaran, and Siegfried Bajohr. 2016. "Review on methanation – From fundamentals to current projects." *Fuel* 166: 276-296.

Schaaf, Tanja, Jochen Grünig, Markus Roman Schuster, Tobias Rothenfluh, and Andreas Orth. 2014. "Methanation of CO2 - storage of renewable energy in a gas distribution system." *Energy, Sustainability and Society* 4 (1).

Seemann, Martin, and Henrik Thunman. 2019. "Methane synthesis." In *Substitute Natural Gas from Waste*, 221-243.

Stangeland, Kristian, Dori Kalai, Hailong Li, and Zhixin Yu. 2017. "CO2 Methanation: The Effect of Catalysts and Reaction Conditions." *Energy Procedia* 105: 2022-2027.

Su, Xiong, Jinghua Xu, Binglian Liang, Hongmin Duan, Baolin Hou, and Yanqiang Huang. 2016. "Catalytic carbon dioxide hydrogenation to methane: A review of recent studies." *Journal of Energy Chemistry* 25 (4): 553-565.

Tada, S., T. Shimizu, H. Kameyama, T. Haneda, and R. Kikuchi. 2012. "Ni/CeO2 catalysts with high CO2 methanation activity and high CH4 selectivity at low temperatures." *International Journal of Hydrogen Energy* 37 (7): 5527-5531.

Upham, D. C., A. R. Derk, S. Sharma, H. Metiu, and E. W. McFarland. 2015. "CO2 methanation by Ru-doped ceria: the role of the oxidation state of the surface." *Catalysis Science & Technology* 5 (3): 1783-1791.

Veselovskaya, Janna V., Pavel D. Parunin, and Aleksey G. Okunev. 2017. "Catalytic process for methane production from atmospheric carbon dioxide utilizing renewable energy." *Catalysis Today* 298: 117-123.

Wang, X. L., T. Zhen, and C. C. Yu. 2016. "Application of Ni-Al-hydrotalcite-derived catalyst modified with Fe or Mg in CO2 methanation." *Applied Petrochemical Research* 6 (3): 217-223.

Wei Wang, Shengping Wang, Xinbin Ma, Jinlong Gong. 2011. "Recent advances in catalytic hydrogenation of carbon dioxide." *CHEMICAL SOCIETY REVIEWS* 40 (7): 3703-3727.

Wierzbicki, D., M. Motak, T. Grzybek, M. E. Galvez, and P. Da Costa. 2018. "The influence of lanthanum incorporation method on the performance of nickel-containing hydrotalcite-derived catalysts in CO2 methanation reaction." *Catalysis Today* 307: 205-211.

Xu, Leilei, Haoming Yang, Mindong Chen, Fagen Wang, Dongyang Nie, Lu Qi, Xinbo Lian, Hanxiang Chen, and Mei Wu. 2017. "CO2 methanation over Ca doped ordered mesoporous Ni-Al composite oxide catalysts: The promoting effect of basic modifier." *Journal of CO2 Utilization* 21: 200-210.

Xu Xiaoding, J. A. Moulijn. 1996. "Mitigation of CO2 by chemical conversion: Plausible chemical reactions and promising products." *ENERGY & FUELS* 10 (2): 305-325.

Yang, Wen, Yanyan Feng, and Wei Chu. 2016. "Promotion Effect of CaO Modification on Mesoporous Al2O3-Supported Ni Catalysts for CO2Methanation." *International Journal of Chemical Engineering* 2016: 1-7.

Zhang, Zhanming, Yue Tian, Lijun Zhang, Song Hu, Jun Xiang, Yi Wang, Leilei Xu, Qing Liu, Shu Zhang, and Xun Hu. 2019. "Impacts of nickel loading on properties, catalytic behaviors of Ni/γ–Al2O3 catalysts and the reaction intermediates formed in methanation of CO2." *International Journal of Hydrogen Energy* 44 (18): 9291-9306.

APPENDICES

APPENDIX A

XRD Patterns of 1,5 And 10 wt.% Ni Loaded 70Al-30Ca-700 Catalysts

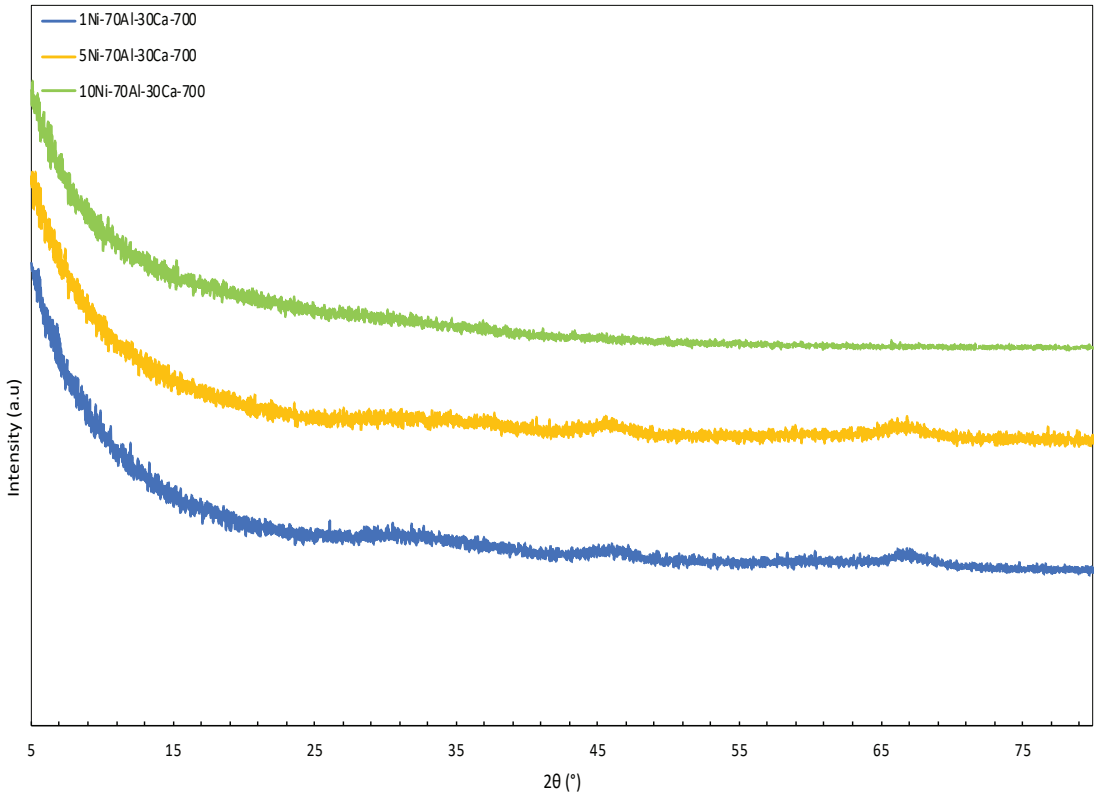

APPENDIX B

Calculations of 10 min. and 45 min. Experiments with 10Ni-10Al-90Ca-700 Catalyst

10 min. of reaction

COMPONENT	Qin (L/min)	Fin (mol/min)	Qout(L/min)	Qout(L/min)	Fout (mol/min)	XCO2	SCH4	YCH4	Carbon Deposition	CO Selectivity
H2	8.17E-02	3.34E-03	4.82E-02	2.13E-02	8.71E-04	84.50%	58.20%	49.18%	33.66%	1.96%
CO	0.00E+00	0.00E+00		3.65E-04	1.49E-05					
CH4	0.00E+00	0.00E+00		1.08E-02	4.42E-04					
CO2	2.20E-02	8.99E-04		3.41E-03	1.39E-04					
Total Carbon		8.99E-04			5.97E-04					

45 min. of reaction

COMPONENT	Qin (L/min)	Fin (mol/min)	Qout(L/min)	Qout(L/min)	Fout (mol/min)	XCO2	SCH4	YCH4	Carbon Deposition	CO Selectivity
H2	8.17E-02	3.34E-03	5.00E-02	3.34E-02	1.37E-03	75.58%	78.77%	59.54%	13.15%	3.83%
CO	0.00E+00	0.00E+00		6.37E-04	2.60E-05					
CH4	0.00E+00	0.00E+00		1.31E-02	5.35E-04					
CO2	2.20E-02	8.99E-04		5.37E-03	2.20E-04					
Total Carbon		8.99E-04			7.81E-04					